Since January 2020 Elsevier has created a COVID-19 resource centre with free information in English and Mandarin on the novel coronavirus COVID-19. The COVID-19 resource centre is hosted on Elsevier Connect, the company's public news and information website.

Virology 397 (2010) 285–298

Contents lists available at ScienceDirect

Virology

journal homepage: www.elsevier.com/locate/yviro

Human parainfluenza virus type 2 V protein inhibits interferon production and signaling and is required for replication in non-human primates

Anne Schaap-Nutt [a,*], Christopher D'Angelo [a], Margaret A. Scull [b,c], Emerito Amaro-Carambot [a], Machiko Nishio [d], Raymond J. Pickles [b,c], Peter L. Collins [a], Brian R. Murphy [a], Alexander C. Schmidt [a]

[a] Laboratory of Infectious Diseases, RNA Viruses Section, National Institute of Allergy and Infectious Diseases, National Institutes of Health, Department of Health and Human Services, Bethesda, MD 20892, USA
[b] Department of Microbiology and Immunology, University of North Carolina at Chapel Hill, Chapel Hill, NC 27599-7248, USA
[c] Cystic Fibrosis/Pulmonary Research and Treatment Center, University of North Carolina at Chapel Hill, Chapel Hill, NC 27599-7248, USA
[d] Department of Microbiology, Mie University Graduate School of Medicine,2-174, Edobashi, Tsu, Mie, 514-8507, Japan

ARTICLE INFO

Article history:
Received 27 July 2009
Returned to author for revision
19 August 2009
Accepted 10 November 2009
Available online 7 December 2009

Keywords:
Parainfluenza virus
V protein
Interferon
Human airway epithelial cultures
Non-human primates

ABSTRACT

In wild-type human parainfluenza virus type 2 (WT HPIV2), one gene (the P/V gene) encodes both the polymerase-associated phosphoprotein (P) and the accessory V protein. We generated a HPIV2 virus (rHPIV2-V^{ko}) in which the P/V gene encodes only the P protein to examine the role of V in replication in vivo and as a potential live attenuated virus vaccine. Preventing expression of V protein severely impaired virus recovery from cDNA and growth in vitro, particularly in IFN-competent cells. rHPIV2-V^{ko}, unlike WT HPIV2, strongly induced IFN-β and permitted IFN signaling, leading to establishment of a robust antiviral state. rHPIV2-V^{ko} infection induced extensive syncytia and cytopathicity that was due to both apoptosis and necrosis. Replication of rHPIV2-V^{ko} was highly restricted in the respiratory tract of African green monkeys and in differentiated primary human airway epithelial (HAE) cultures, suggesting that V protein is essential for efficient replication of HPIV2 in organized epithelial cells and that rHPIV2-V^{ko} is over-attenuated for use as a live attenuated vaccine.

Published by Elsevier Inc.

Introduction

Human parainfluenza virus serotypes 1, 2 and 3 (HPIV1-3) are negative-stranded, non-segmented, enveloped RNA viruses that belong to the Paramyxoviridae family. These HPIVs are a major cause of respiratory illness in children and account for 18% of pediatric hospitalizations for acute respiratory tract infection (Murphy, 1988). HPIV disease ranges from mild upper respiratory tract illness (URTI) to severe lower respiratory tract disease, including croup, bronchiolitis and pneumonia. HPIV2 is thought to be an important cause of URTI, croup, and undifferentiated febrile illness (Kapikian et al., 1963; Parrott et al., 1962). Currently, there are no effective antiviral therapies or vaccines to treat or prevent HPIV infections.

Unlike HPIV1 and HPIV3, which are both members of the genus *Respirovirus*, HPIV2 is a *Rubulavirus*. It encodes 7 polypeptides from 6 genes arranged in the order 3′-N-P/V-M-F-HN-L-5′. The HPIV2 genome is 15,654 nucleotides in length and requires a genome nucleotide length that is a multiple of six for efficient replication (known as the "rule of six") (Skiadopoulos et al., 2003). Transcription and replication are directed by the viral nucleocapsid protein (N), the phosphoprotein (P), and the large polymerase (L) protein (Karron and Collins, 2007). The fusion (F) and hemagglutinin-neuraminidase (HN) glycoproteins are the major protective antigens for the HPIVs and are associated with the viral envelope, along with the internal matrix protein (M) (Murphy, 1988). The remaining polypeptide, the accessory V protein, has been identified as an antagonist of the type I interferon (IFN) response (Andrejeva et al., 2004; He et al., 2002; Horvath, 2004; Poole et al., 2002; Young et al., 2000).

The P/V gene of HPIV2 encodes both the phosphoprotein P subunit of the viral polymerase and the accessory V protein (Ohgimoto et al., 1990). Unedited transcription of the P/V gene yields an mRNA that codes for the V protein. Alternatively, the co-transcriptional insertion of two non-templated guanine nucleotides by RNA editing generates an mRNA with a frame shift that codes for the P protein. Therefore, P and V proteins share the first 164 N-terminal amino acids but have distinct C-termini. RNA editing to insert pseudotemplated G nucleotides is a conserved viral mechanism that occurs in nearly all members of the five genera in subfamily Paramyxovirinae (Karron and Collins, 2007).

The P protein is an essential component of the viral RNA polymerase with multiple roles in mRNA transcription and genome replication (Lamb and Parks, 2007). The primary function of the V protein appears to be inhibition of the innate antiviral response, though V is also believed to play a part in preventing apoptosis and

* Corresponding author. LID, NIAID, NIH, 50 South Drive, Bldg. 50, Room 6515, MSC 8007, Bethesda, MD 20892-8007, USA. Fax: +1 301 480 1268.
E-mail address: schaapa@niaid.nih.gov (A. Schaap-Nutt).

0042-6822/$ – see front matter. Published by Elsevier Inc.
doi:10.1016/j.virol.2009.11.018

regulating viral RNA synthesis (Didcock et al., 1999b; He et al., 2002; Lin and Lamb, 2000; Poole et al., 2002; Wansley and Parks, 2002). The latter function may be mediated through binding of the V protein to the virus N and L proteins as well as to RNA (Lin et al., 1997; Nishio et al., 2008, 2007, 2006; Randall and Bermingham, 1996). In addition to these functions, the V proteins of rubulaviruses are components of the virions, whereas V has not been detected in the virions of respiroviruses or morbilliviruses (Curran et al., 1991; Paterson et al., 1995). A role for V in virion morphogenesis has been suggested but remains to be defined in detail (Kawano et al., 2001).

The innate immune response is a powerful host defense against virus infection and, as a result, is a target for interference by proteins encoded by many diverse viruses (Fensterl and Sen, 2009; Goodbourn et al., 2000). RNA virus infection is detected by a number of host cell pathogen recognition receptors (PRRs) that induce innate immune responses such as the IFN and apoptotic responses. Toll-like receptors, which are expressed on the cell surface and in endosomes, recognize specific viral products such as viral nucleic acids present in intracellular vesicles or in the extracellular environment, whereas retinoic acid-inducible gene I (RIG-I) and melanoma differentiation-associated gene 5 (MDA5) are constitutively expressed RNA helicases that detect viral RNAs in the cytosol. Activation of either type of PRR signals both IFN-α/β synthesis and subsequent IFN-α/β signaling through its receptor (Koyama et al., 2007; Yoneyama and Fujita, 2007; Yoneyama et al., 2004). IFNs are secreted from most cells and can act in either an autocrine or paracrine manner. The effects of IFN on the host cell are initiated by engagement and multimerization of the IFN-α-receptor (IFNAR) by IFN-α or IFN-β. The IFNAR-associated tyrosine kinases, Tyk2 and Jak1, phosphorylate IFNAR1 and 2 receptor subunits, thereby triggering recruitment, phosphorylation and release of STAT1 and STAT2 from the receptor into the cytoplasm. Activated STAT1 and STAT2 associate with IRF9 to form a complex known as interferon-stimulated gene factor 3 (ISGF3), which translocates to the nucleus and activates transcription of IFN-inducible genes (ISGs). The ISGs establish an antiviral state in both infected and uninfected cells and also serve to augment the adaptive immune response (Fensterl and Sen, 2009).

One attractive strategy that has been proposed for attenuating viruses for use as live virus vaccines involves deleting or mutating IFN antagonists encoded by viruses (Talon et al., 2000). The multifunctional V protein of HPIV2 has been shown to counteract the IFN response at two steps: limiting induction of IFN biosynthesis by viral dsRNA through an interaction with the RNA helicase MDA5 (Andrejeva et al., 2004; Childs et al., 2007) and blocking IFN signaling by engaging STAT1 and STAT2 proteins in a cytoplasmic complex with a cellular E3 ubiquitin ligase, resulting in ubiquitination and proteasomal degradation of STAT2 (Andrejeva et al., 2002; Nishio et al., 2002, 2005). These data suggest that mutation or ablation of HPIV2 V protein could be used as a strategy to generate a live attenuated HPIV2 vaccine candidate. However, as potential complications, abrogation of the IFN-independent function of V on polymerase activity and replication by mutation could result in a reduction in the yield of live vaccine in cell culture during manufacture or in over-attenuation of the vaccine in vivo.

Previously, two recombinant HPIV2 viruses, one with mutations preventing V protein expression entirely and one with mutations creating a V protein with a truncated C-terminal domain, were derived from the Toshiba strain of HPIV2 (Kawano et al., 2001; Nishio et al., 2005). Both mutants were highly restricted for replication in a number of cell lines, including in Vero cells, which cannot produce type I IFNs (Kawano et al., 2001; Nishio et al., 2005). However, the efficiency of growth of these two V mutants in vivo was not reported, and the full genome sequence was not presented. In the present study, we used a rule-of-six-compliant recovery system to generate an independent recombinant HPIV2 (rHPIV2-V^{ko}) in which V expression was ablated by the introduction of alterations in the RNA editing site of the P/V gene, similar to the HPIV2 mutant generated by Nishio et al. (2005). Sequence analysis of recovered rHPIV2-V^{ko} virus confirmed that it had a wild-type sequence in all expressed proteins (Skiadopoulos et al., 2003) and that rHPIV2-V^{ko} contained only one incidental mutation in a noncoding region judged to be biologically insignificant. This study extends the previous observations by examining the ability of rHPIV2-V^{ko} to induce the synthesis of IFN, to inhibit IFN signaling through its receptor, to replicate in vivo in non-human primates, and to replicate in human well-differentiated primary airway epithelial cells in culture. rHPIV2-V^{ko} was found to be restricted for growth in vitro due to enhanced cytopathic effect (CPE) and an inability to antagonize both the induction of IFN and IFN signaling through its receptor. These defects proved to be highly restrictive for growth in African green monkeys (AGMs) and in cultures of human ciliated airway epithelium (HAE).

Results

Construction and recovery of rHPIV2 that does not express V protein

In wild-type (WT) HPIV2, the P and V mRNAs are encoded by overlapping reading frames, as illustrated in Fig. 1A. HPIV2 and other paramyxoviruses use a unique mechanism of mRNA editing to insert pseudotemplated G residues during transcription of the P gene. Upon reading a specific editing site (depicted in Fig. 1A), the viral polymerase occasionally "stutters," slippage of the nascent mRNA occurs, and one or more extra G nucleotides are added. In P genes from genus *Respiro-*, *Avula-*, *Henipa-* and *Morbillivirus*, the unedited mRNA encodes P, while insertion of one G residue produces V mRNA. The opposite occurs in the *Rubulaviruses*, where the unedited mRNA encodes V and the edited version encodes P via a two-nucleotide frame shift (Fig. 1A). Other groups have previously demonstrated that it is possible to prevent HPIV2 V protein expression by mutating the RNA editing site in the P/V gene (Kawano et al., 2001; Nishio et al., 2005). Using our reverse genetics system that is based on the sequence of a low passage HPIV2 clinical isolate that replicates to high titer in non-human primates (Nolan et al., 2007), we altered the P/V editing site to create the two-nucleotide frame shift, so that the unedited mRNA encodes only P, and disrupted the string of G nucleotides by substitution mutagenesis in order to inactivate editing (Fig. 1B). This was done without introducing any coding mutations into P.

We observed that this recombinant virus (rHPIV2-V^{ko}) had a lower frequency of recovery from cDNA than rHPIV2-WT in IFN-competent HEp-2 cells. rHPIV2-V^{ko} was recovered in 5 out of 12 transfections (42% recovery rate) whereas rHPIV2-WT was recovered in all 12 transfections (100% recovery). One of the five recovered rHPIV2-V^{ko} populations had an editing site that was restored exactly to that of the WT virus, though other introduced sequence changes (e.g., restriction sites) were present in the sequence of the recovered virus (Table 1, mutant 5). Another mutant (Table 1, mutant 4) had an editing site that was restored to that of the WT virus except that it was three G residues longer; thus, its P editing site had gained a single nucleotide in length compared with the original V^{ko} mutant sequence, and this gain appeared to be compensated for by a single-nucleotide deletion in the poly(A) tract at the end of the N gene-end signal (Table 1, mutant 4). A third mutant had ten T to C mutations between the open reading frames of N and P that highly impaired its growth in vitro (Table 1, mutant 3). The final two recovered rHPIV2-V^{ko} isolates had P editing sites that retained all of the mutations of the original V^{ko} mutant, although both contained a single, different nucleotide substitution in the gene-end signal of the N gene (Table 1, mutants 1 and 2). Mutant 2 contained a T to A substitution at nucleotide (nt) 1912 in the N gene-end signal, whose phenotypic consequences were not investigated. The N gene-end region was a site of adventitious mutations in 4 of the 5 recovered rHPIV2-V^{ko} isolates and is therefore

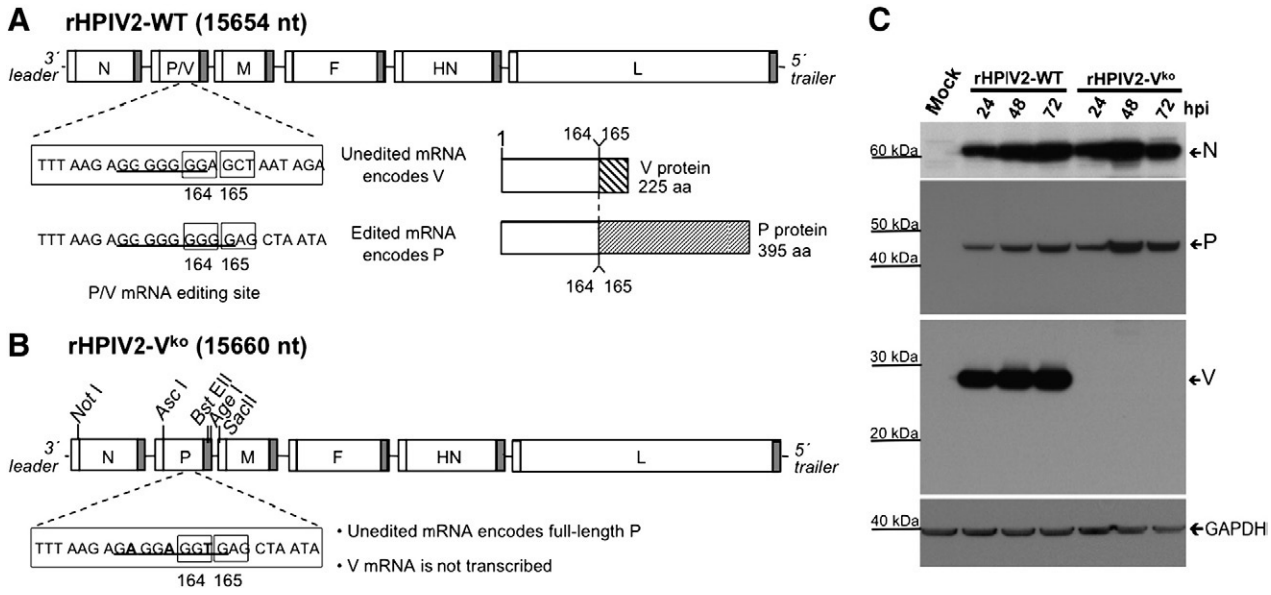

Fig. 1. Generation of rHPIV2 that does not express the V protein. (A) Schematic representation of the wild-type (WT) HPIV2 genome. The nucleotide sequence at the P/V mRNA editing site is shown for both the P and V mRNAs with underlined nucleotides denoting the sites of seven (V mRNA) or nine (P mRNA) G residues. As indicated, the P and V proteins share identical N-terminal sequences but have unique C-terminal sequences after the editing site. (B) Diagram of HPIV2 cDNA used to recover infectious rHPIV2-V^{ko}. The unique, silent restriction enzyme sites *Asc*I, *Bst*EII, *Age*I, and *Sac*II were introduced in order to alter the editing site in the P gene. The nucleotide sequence of the mRNA editing site in the P ORF is shown with the three nucleotide substitutions introduced to disable the editing site presented in bold. (C) Expression of HPIV2 proteins in LLC-MK2 cells mock-infected or infected with rHPIV2-WT or rHPIV2-V^{ko}. Cells were infected at an MOI of 5.0 $TCID_{50}$/cell and lysed at 24, 48, and 72 h post-infection (hpi). Protein expression was analyzed by SDS–PAGE and immunoblotting with antibodies to HPIV2 N, P and V proteins and cellular GAPDH, which serves as a loading control.

included in Table 1. Mutant 1 contained an A to G substitution at nucleotide 1917, which changed the length of the poly(A) tract in the gene-end signal from 7 to 6 residues. Mutations or natural variation affecting the length of the poly(A) sequence of the gene-end signal are common for paramyxoviruses in general and usually are without phenotypic consequences (Collins and Crowe, 2007; Kolakofsky et al., 1998; Rassa et al., 2000), and therefore mutant 1 was analyzed further. Western blot analysis revealed that expression of the gene downstream of the gene-end mutation, encoding P protein, is at least equivalent to expression of P in rHPIV2-WT-infected cells (Fig. 1C). At 24, 48, and 72 h post-infection (hpi), both HPIV2 N and P proteins were expressed efficiently by rHPIV2-V^{ko} (Fig. 1C), indicating that the mutation in the gene-end sequence of rHPIV2-V^{ko} does not functionally impair mRNA synthesis and can be considered an incidental mutation of little biological significance. rHPIV2-V^{ko} replicated efficiently in vitro, and sequence analysis of its entire genome showed that it was free of any additional adventitious mutations. Western blot analysis of infected LLC-MK2 cell lysates using antibodies directed against both the N- and C-termini of the HPIV2 V protein confirmed that rHPIV2-V^{ko} did not express the V protein (Fig. 1C). In addition, smaller bands were not detected in either rHPIV2-WT or rHPIV2-V^{ko} with antibodies specific to the N-terminus of P/V, while V and P were readily detected, indicating that neither virus expresses a W protein and that the alterations in the editing site prevent expression of C-terminally truncated V or W proteins. Therefore, this isolate was used throughout the remainder of the study as rHPIV2-V^{ko}.

Table 1
Sequence analysis of recovered rHPIV2-V^{ko}.

Virus	Nucleotide Sequence[a]		Comment
	N gene end[b]	P editing site[c]	
HPIV2-WT	CTCCTAGAATTTAAGAAAAAACAT	TAAGAGGGGGGG--AGCTA	WT cDNA sequence
HPIV2-V^{ko}	CTCCTAGAATTTAAGAAAAAACAT	TAAGAG**A**GG**A**GG**TG**AGCTA[d]	V^{ko}cDNA sequence
Recovered rHPIV2-V^{ko}mutants[e]			
1	CTCCTAGAATTTAAGGAAAAAACAT	TAAGAG**A**GG**A**GG**TG**AGCTA	Contains V^{ko} P editing site[f]
2	CTCCTAGAATTAAAGAAAAAACAT	TAAGAG**A**GG**A**GG**TG**AGCTA	ContainsV^{ko} P editing site
3	CCCCCAGAATCCAAGAAAAAACAT	TAAGAG**A**GG**A**GG**TG**AGCTA	Ten T to C mutations
4	CTCCTAGAATTTAAGAAAAAA-CAT	TAAGAGGGGGGGGGAGCTA	P editing site mutation
5	CTCCTAGAATTTAAGAAAAAACAT	TAAGAGGGGGGAGCTA	P editing site reversion

[a] Antigenomic sense nucleotide sequence of selected regions of HPIV2 genome.
[b] Adventitious mutations were frequently noted in the N gene-end sequence of recovered rHPIV2-V^{ko} mutants. The gene-end sequence is boxed.
[c] Sequence of the P editing site of recovered viruses compared to the HPIV2-V^{ko} cDNA sequence used for virus recovery.
[d] The P editing site mutations to create HPIV2-V^{ko} are indicated by bold type.
[e] Sequences of viruses recovered from HPIV2-V^{ko} cDNA from five transfections. Underlined nucleotides indicate adventitious mutations.
[f] Recovered rHPIV2-V^{ko} clone no. 1 is shaded to indicate that this virus was used for all experiments in the study.

rHPIV2-V^{ko} exhibits restricted replication and spread in vitro

Single and multi-cycle replication of rHPIV2-V^{ko} was assessed in A549, Vero, and LLC-MK2 cells infected at an MOI of 5.0 or 0.01 $TCID_{50}$/cell, respectively (Fig. 2A and B). In A549 cells, a human type II pneumocyte cell line, rHPIV2-V^{ko} replicated poorly and reached a peak titer of 3.0 $\log_{10}TCID_{50}$/ml following high MOI inoculation, 100-fold lower than the peak titer of rHPIV2-WT (peak titer 5.0 $\log_{10}TCID_{50}$/ml). Similarly, rHPIV2-V^{ko} reached a peak titer of 3.6 $\log_{10}TCID_{50}$/ml following low MOI inoculation, 630-fold lower than the peak titer of rHPIV2-WT (peak titer 6.4 $\log_{10}TCID_{50}$/ml). Furthermore, titers of rHPIV2-V^{ko} reached a plateau after 2 days post-infection (p.i.), while titers of rHPIV2-WT increased through day 8 p.i. Replication of rHPIV2-V^{ko} was also evaluated in two monkey cell lines (Fig. 2A and B). African green monkey Vero cells were selected because they are unable to produce type I interferon (IFN) and because they would be the substrate used to manufacture a live attenuated HPIV2 vaccine. IFN-competent LLC-MK2 rhesus monkey kidney cells were chosen because rHPIV2-WT replicates efficiently in this cell line. rHPIV2-V^{ko} replication was only slightly restricted

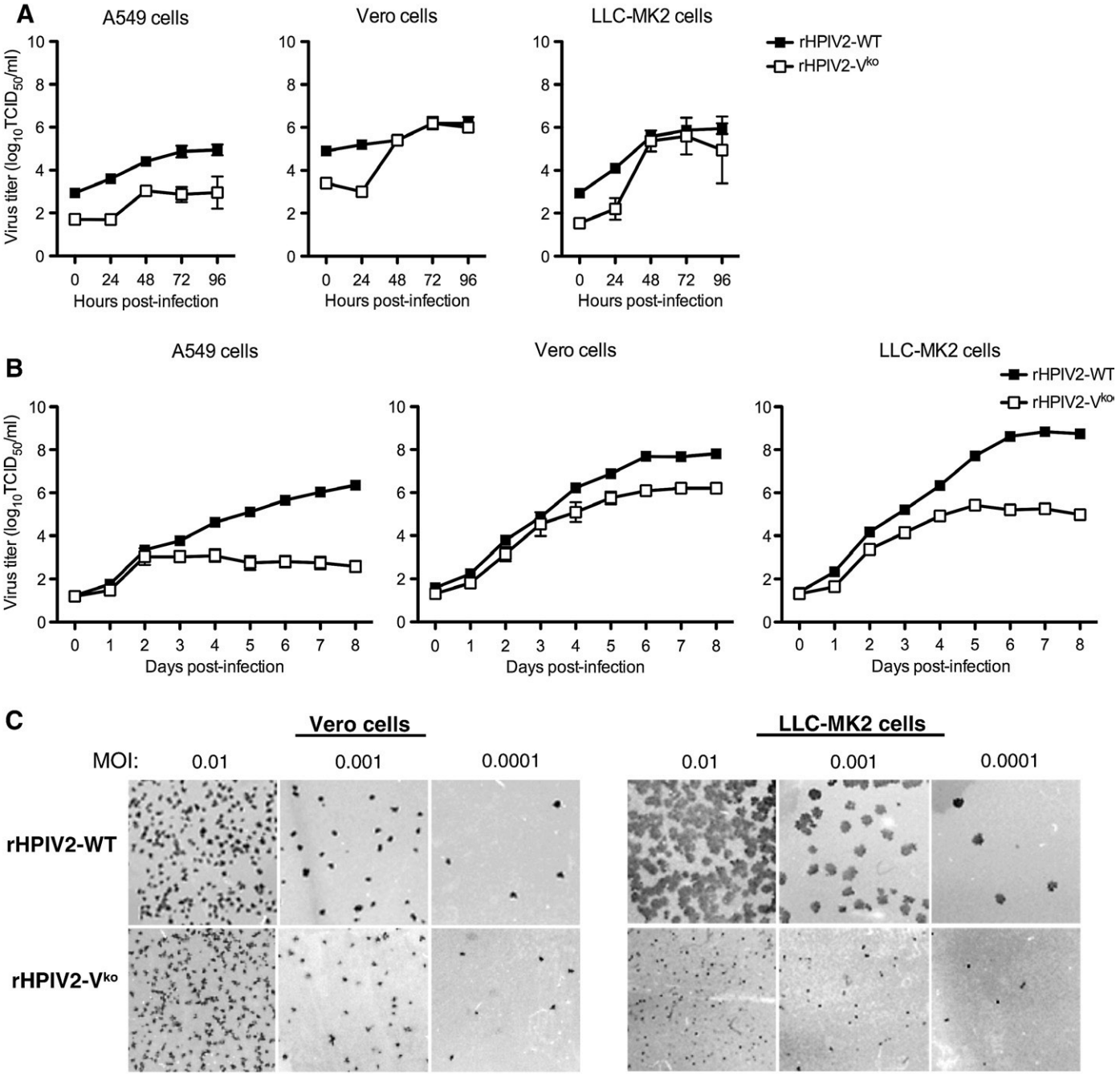

Fig. 2. Comparison of the growth of rHPIV2-WT and rHPIV2-V^{ko} in vitro in IFN-competent (A549 and LLC-MK2) and IFN-lacking (Vero) cells. Single-cycle (A) or multi-cycle (B) replication of rHPIV2-WT (filled squares) or rHPIV2-V^{ko} (open squares) in A549, Vero, or LLC-MK2 cells. Triplicate cell cultures in 6-well plates were infected at an MOI of 5.0 (A) or 0.01 (B) $TCID_{50}$/cell with each virus. Aliquots of culture media replaced at 24-h intervals were titrated by 10-fold serial dilution on LLC-MK2 cells and scored by hemadsorption. The mean virus titer for each time point is expressed as $\log_{10}TCID_{50}/ml \pm SE$. (C) Plaque size comparison between rHPIV2-WT and rHPIV2-V^{ko}. Monolayers of Vero cells (left panels) or LLC-MK2 cells (right panels) were infected with the indicated viruses at an MOI of 0.01, 0.001, or 0.0001 $TCID_{50}$/cell. Cells were overlaid with 0.8% methylcellulose, incubated at 32 °C for 10 days p.i., then fixed in methanol. Plaques were stained with polyclonal anti-HPIV2 rabbit immune serum and developed with horseradish peroxidase-conjugated anti-rabbit antibodies and peroxidase substrate. Plaques were imaged without magnification.

following high MOI inoculation but was significantly restricted in both Vero and LLC-MK2 cells compared with rHPIV2-WT following low MOI inoculation ($p<0.001$, two-way ANOVA with Bonferroni post-tests). In multi-cycle growth curves, replication of rHPIV2-V^{ko} was restricted 50-fold in Vero cells (peak titer 6.4 $\log_{10}$TCID$_{50}$/ml) and 2500-fold in LLC-MK2 cells (peak titer 5.4 $\log_{10}$TCID$_{50}$/ml) compared with rHPIV2-WT (peak titer 8.1 $\log_{10}$TCID$_{50}$/ml in Vero cells and 8.8 $\log_{10}$TCID$_{50}$/ml in LLC-MK2 cells). Sequence analysis of rHPIV2-V^{ko} isolated from cell cultures after completion of the growth curves confirmed that the mutations introduced into the P/V editing site remained intact. These data indicate that the growth of rHPIV2-V^{ko} is significantly restricted in vitro, although to a lesser extent in the absence of a cellular IFN response. The sensitivity of replication of rHPIV2-V^{ko} to elevated temperatures (37–40 °C) was also evaluated in vitro to determine whether the V deletion altered the stability of the replication complex. Replication at 37–39 °C was comparable to that at 32 °C but was restricted >100-fold at 40 °C (data not shown), indicating a temperature sensitivity of replication at or above 40 °C.

In order to assess the cell-to-cell spread of rHPIV2-V^{ko}, we infected monolayers of Vero and LLC-MK2 cells with serial dilutions of virus using a methylcellulose overlay (Fig. 2C). Following incubation for 10 days, plaques were visualized by immunostaining with HPIV2-specific antibodies, and plaque sizes were compared between rHPIV2-WT and rHPIV2-V^{ko}. In Vero cells, rHPIV2-V^{ko} plaques were approximately 37% smaller than rHPIV2-WT plaques (2.4 ± 0.2 pixels for rHPIV2-V^{ko} versus 3.8 ± 0.2 for rHPIV2-WT, $p<0.001$). In LLC-MK2 cells, a more dramatic reduction (94%) in the plaque size of rHPIV2-V^{ko} was observed compared with rHPIV2-WT (0.8 ± 0.1 versus 13.5 ± 1.0, $p<0.001$). Thus, rHPIV2-V^{ko} exhibits a small plaque phenotype that is particularly pronounced in IFN-competent LLC-MK2 cells, but also is apparent to a lesser extent in IFN-lacking Vero cells. Plaque size was not assessed in A549 cells due to the overall poor multi-cycle replication of rHPIV2-V^{ko} in this cell line.

rHPIV2-V^{ko} causes increased CPE compared to rHPIV2-WT

In the course of determining the replication kinetics of rHPIV2-V^{ko}, we observed that this mutant caused more syncytia formation and CPE than rHPIV2-WT in LLC-MK2 and Vero cells. To further investigate this phenomenon, LLC-MK2 cells were infected at high MOI (5.0 TCID$_{50}$/cell), and CPE was inspected by microscopy. rHPIV2-V^{ko} caused extensive syncytia formation by 48 hpi, followed by CPE that destroyed the infected cell monolayers by 72 hpi (Fig. 3A). In contrast, rHPIV2-WT did not cause significant CPE in any of the cell lines, and syncytia did not form in LLC-MK2 cells until 7–8 days p.i. (Fig. 3A and data not shown). CPE was not visible for either virus in A549 cells, possibly due to the poor replication of rHPIV2-V^{ko} in this cell line.

Recently, a mutant of HPIV1 that does not express the IFN antagonist C proteins, rHPIV1-P(C−), was shown to cause extensive CPE within a few days of infection in vitro, in contrast to the non-cytopathic WT HPIV1, and this CPE was associated with extensive apoptosis (Bartlett et al., 2008a). Since the V proteins of PIVs have been reported to inhibit apoptosis (Sun et al., 2004; Wansley and Parks, 2002) and since the CPE induced looked similar to that observed for rHPIV1-P(C−), we next explored whether the CPE induced by rHPIV2-V^{ko} might also be due to apoptosis. In these experiments, we used the HPIV1 viruses as positive (rHPIV1-P(C−)) or negative (WT HPIV1) controls for apoptosis. We determined the frequency of apoptosis in infected cells using flow cytometry to detect activated caspase-3, the major effector caspase in the apoptotic pathway. Replicate cultures of LLC-MK2 cells were infected with rHPIV2-WT, rHPIV2-V^{ko}, or the HPIV1 control viruses at an MOI of 5.0 TCID$_{50}$/cell and were fixed at 24, 48, and 72 hpi. Cells were then permeabilized and immunostained for activated caspase-3. As described previously, rHPIV1-P(C−) was a potent inducer of caspase-3 activation while rHPIV1-WT was not (Fig. 3B). Specifically, in cultures infected with rHPIV1-WT, less than 1.2% of the cells expressed activated caspase-3 through 72 hpi, which was similar to mock-infected cultures (approximately 0.5% positive for activated caspase-3). In contrast, in cultures infected with the rHPIV1-P(C−) positive control, greater than 50% of the cells at 48 and 72 hpi expressed activated caspase-3, indicative of cells undergoing apoptosis. rHPIV2-WT caused slightly more apoptosis than rHPIV1-WT, with 7.1% of cells expressing activated caspase-3 at 72 hpi ($p<0.001$). Unexpectedly, in rHPIV2-V^{ko}-infected cultures, there was only a small (2-fold) increase in activated caspase-3-positive cells (14.2% at 72 hpi) compared to rHPIV2-WT. While this increase was statistically significant ($p<0.001$), we had expected a substantially larger increase given the extent of cell destruction that was evident from light microscopic evaluation (Fig. 3A). Extensive cell destruction also was evident from the decrease in the forward scatter parameter for events measured by FACS analysis of rHPIV2-V^{ko}-infected cultures (Fig. 3B), which indicates reduced cell size and accumulation of cell debris. These results suggested that the majority of cells infected with rHPIV2-V^{ko} were not dying through an apoptotic pathway.

Because antibody against activated caspase-3 has the potential to bind non-specifically to necrotic cells, leading to an overestimation of the percent apoptotic cells, we confirmed cleavage activation of caspase-3 by immunoblot analysis of infected LLC-MK2 cell lysates (Fig. 3C). As we observed by flow cytometric detection of activated caspase-3, the cleaved (activated) form of caspase-3 was detected by immunoblot at 48 and 72 h after infection with rHPIV2-V^{ko} or rHPIV1-P(C−). Cleaved caspase-3 was also detected to a lesser extent in cells infected with rHPIV2-WT, though not rHPIV1-WT, correlating with results seen by flow cytometry.

We next evaluated cytotoxicity by the quantification of plasma membrane damage. One ubiquitous intracellular enzyme that is rapidly released into culture medium only upon damage to the plasma membrane is lactate dehydrogenase (LDH); therefore, measuring activity of LDH released into the culture media allows rapid quantification of cells whose plasma membrane has been damaged by cytotoxic effect. An increase in the level of LDH activity in the culture media is proportional to the number of dead or damaged cells in the culture. When we measured LDH release from LLC-MK2 cells at 24, 48, and 72 hpi, we found that rHPIV2-V^{ko} induced approximately 40% more LDH release at 72 hpi than rHPIV2-WT or, surprisingly, rHPIV1-P(C−) (Fig. 3D). We conclude from these data that rHPIV2-V^{ko} exhibits a marked increase in its ability to induce cell–cell fusion and cytopathicity compared to rHPIV2-WT. However, unlike rHPIV1-P(C−), rHPIV2-V^{ko} appears to cause CPE primarily through syncytia formation and necrosis rather than through the induction of apoptosis, although both processes are active during infection with rHPIV2-V^{ko}.

One possible explanation for the early appearance (day 2) of syncytia in rHPIV2-V^{ko}-infected cells is that F and HN may accumulate in the plasma membrane more rapidly than in rHPIV2-WT-infected cells and enhance cell–cell fusion. To quantify expression of F and HN on the plasma membrane, we stained live adherent LLC-MK2 cells for cell surface expression of HPIV2 F and HN and estimated the level of expression by FACS analysis. We chose this method because it would allow us to compare the relative amount of F and HN glycoprotein incorporated into the infected cell membranes without involuntarily analyzing intracellular F and HN. Using this technique, no significant difference in mean fluorescence intensity (MFI) was detected for F at 24 hpi (MFI of 60.3 for rHPIV2-WT vs. 51.4 for rHPIV2-V^{ko}) or 48 hpi (MFI of 87.0 for rHPIV2-WT vs. 80.1 for rHPIV2-V^{ko}). Similarly, the MFI for HN protein was comparable between cells infected with either of the two viruses at both 24 hpi (MFI of 357 for rHPIV2-WT vs. 338 for rHPIV2-V^{ko}) and 48 hpi (MFI of 363 for rHPIV2-WT vs. 405 for rHPIV2-V^{ko}). Since we were unable to detect a difference in cell

surface glycoprotein expression, we conclude that factors in addition to the level of F and HN expression likely play a major role in syncytia formation. However, these data and interpretations are offered with the caveat that infection with rHPIV2-V^{ko} is a dynamic process where some cells form syncytia and others detach or die, adding uncertainly into the interpretation of the F and HN expression data.

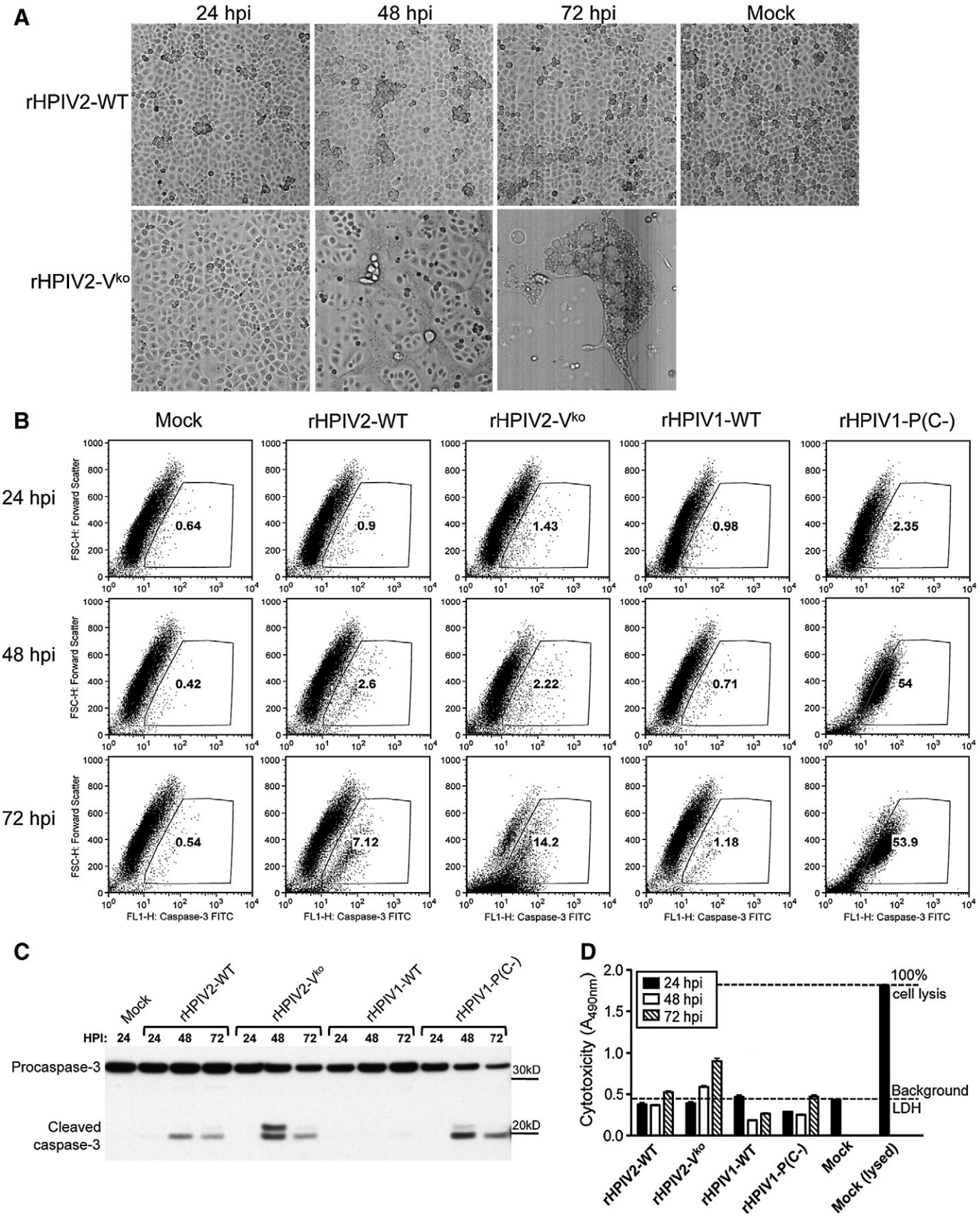

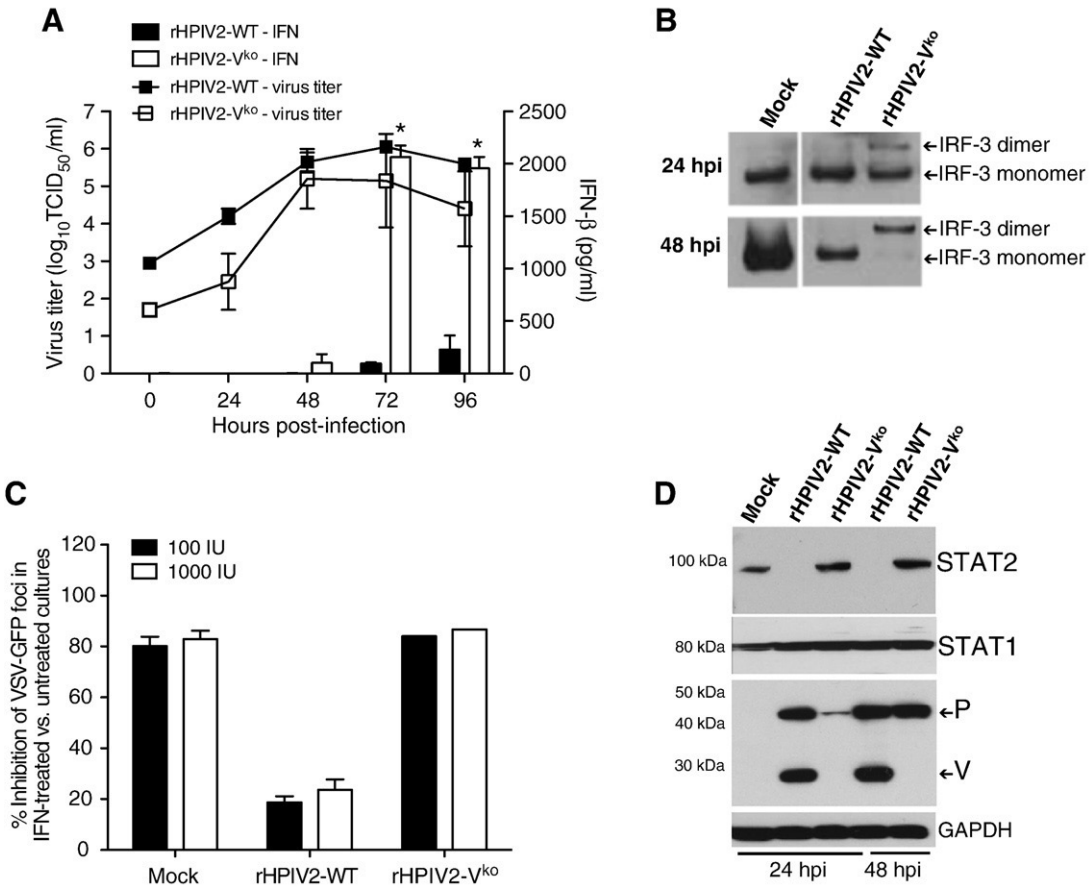

Fig. 4. IFN induction and signaling in response to HPIV2 infection. (A) IFN-β induction during infection with rHPIV2-WT and rHPIV2-V^{ko}. LLC-MK2 cells were infected with rHPIV2-WT (filled boxes) or rHPIV2-V^{ko} (open boxes) at an MOI of 5.0 $TCID_{50}$/cell. The culture medium was replaced at 0, 24, 48, 72, and 96 hpi and aliquots were analyzed to determine virus titer and ELISA IFN-β levels. Bar graphs show IFN-β concentrations (scale on right *Y*-axis), which were determined by comparison with an IFN-β standard curve and are expressed in pg/ml ± SE based on results for triplicate samples from two independent experiments. Asterisks indicate samples in which IFN-β levels were significantly higher than in rHPIV2-WT-infected culture supernatant at the same time point ($p<0.001$). The lower limit of detection was 12 pg/ml. Line graphs show the virus titer (scale on left *Y*-axis) for each sample, determined by 10-fold serial dilution of the culture supernatant on LLC-MK2 cells. Mean daily virus titers are expressed as $\log_{10}TCID_{50}$/ml ± SE. (B) IRF-3 dimerization in HPIV2-infected LLC-MK2 cells. Cells were mock-infected or infected with rHPIV2-WT or rHPIV2-V^{ko} at an MOI of 5.0 $TCID_{50}$/cell and lysed at 24 and 48 hpi. Cell lysates were resolved by PAGE electrophoresis under native conditions, and immunoblot was used to identify both monomeric and dimeric forms of IRF-3. (C) Type I IFN signaling during infection with rHPIV2-WT and rHPIV2-V^{ko}. Vero cells in six-well plates were mock-infected or infected with rHPIV2-WT or rHPIV2-V^{ko} at an MOI of 5.0 $TCID_{50}$/cell for 24 h. Cells were then left untreated or were treated with 100 or 1000 IU/ml IFN-β (2 cultures per treatment per virus). After 24 h, the cells were infected with VSV-GFP and incubated for 48 h. A phosphorimager was used to visualize the VSV-GFP foci. The graph represents the percent inhibition of VSV-GFP foci (± SE) in IFN-β-treated versus untreated cells. (D) STAT2 protein degradation. Vero cells infected at an MOI of 5.0 $TCID_{50}$/cell were lysed at 24 or 48 hpi and analyzed by SDS–PAGE and immunoblotted for STAT2, STAT1, and GAPDH (loading control) cellular proteins and for P and V viral proteins.

rHPIV2-V^{ko} exhibits enhanced IFN-β production

HPIV2 V protein has been shown to directly bind to the cytosolic dsRNA sensor MDA5 and to inhibit production of IFN-β in response to viral infection (Andrejeva et al., 2004; Childs et al., 2007). Although the importance of MDA5 inhibition for sensing paramyxovirus infection has not yet been well defined, we sought to determine the effect of deleting V protein on the ability of HPIV2 to block IFN-β induction during infection. LLC-MK2 cells were infected at an MOI of 5.0 $TCID_{50}$/cell with rHPIV2-WT or rHPIV2-V^{ko}, and the concentration of IFN-β in the culture supernatant was determined by an ELISA that detects active IFN-β (Fig. 4A). A low level of IFN-β was detected in response to rHPIV2-WT infection of LLC-MK2 cells (95 pg/ml at 72 hpi and 228 pg/ml at 96 hpi). In contrast, cells infected with rHPIV2-V^{ko} showed markedly increased IFN-β production by 72 hpi (20-fold over rHPIV2-WT). Similar results were found using a type I IFN bioassay based on the inhibition of plaque formation by VSV-GFP (data not shown). Unlike rHPIV2-WT, rHPIV2-V^{ko} appears to be unable to inhibit the production of IFN-β by infected cells.

Fig. 3. Comparison of CPE, caspase-3 activation, and cytotoxicity induced by infection with rHPIV2-WT or rHPIV2-V^{ko}. (A) Confluent monolayers of LLC-MK2 cells were mock-infected or infected with rHPIV2-WT or rHPIV2-V^{ko} at an MOI of 5.0 $TCID_{50}$/cell. Syncytium formation and cell death are apparent by 48 h after infection with rHPIV2-V^{ko}. Photomicrographs taken at 72 hpi show increased CPE in rHPIV2-V^{ko}-infected cultures. Mock cultures appeared like those of rHPIV2-WT. (B) Evaluation of caspase-3 activation by FACS analysis. LLC-MK2 cells were mock-infected or infected with the indicated viruses at an MOI of 5.0 $TCID_{50}$/cell, including rHPIV1-WT and rHPIV1-P(C−) viruses as negative and positive controls. At 24, 48, and 72 hpi, cells were fixed, permeabilized, and stained for activated caspase-3. Dot plots are representative of data for triplicate samples from two independent experiments. Gates indicate the population of cells (% of total events) positive for activated caspase-3 at each time point as determined by FACS analysis. (C) Immunoblot for caspase-3. LLC-MK2 cells infected at an MOI of 5.0 $TCID_{50}$/cell were lysed at 24, 48, or 72 hpi and then analyzed by SDS–PAGE and caspase-3 immunostaining. Full-length procaspase-3 is approximately 35 kDa and is proteolytically cleaved into activated 17 kDa and 12 kDa fragments. (D) Cytotoxicity was quantified by measuring lactate dehydrogenase (LDH) release from LLC-MK2 cells collected at 24, 48 and 72 hpi. LDH in the culture supernatant activated a colorimetric detection reagent, which was detected using a microplate reader; activity is expressed as absorbance at 490nm. Spontaneous (background) LDH release was determined from culture supernatant from mock-infected cells, while the maximal release of LDH activity was determined from supernatant of a lysed, mock-infected culture.

IFN-β production in response to virus infection is initiated by the transcription factor IRF-3, which is activated by phosphorylation, causing it to dimerize and translocate to the nucleus where it binds to the IFN-β promoter (Yoneyama et al., 1998). To evaluate the dimerization of IRF-3 in response to HPIV2 infection, LLC-MK2 cells were infected with rHPIV2-WT or rHPIV2-V^{ko} at an MOI of 5.0 $TCID_{50}$/cell, and dimerization assays were performed at 24 and 48 hpi. rHPIV2-WT inhibited IRF-3 dimerization, whereas rHPIV2-V^{ko} induced IRF-3 dimerization (Fig. 4B). No IRF-3 dimerization was evident in mock-infected cells. Therefore, dimerization of IRF-3 following rHPIV2-V^{ko} infection correlates well with the high levels of IFN-β production in response to this virus.

rHPIV2-V^{ko} cannot block IFN signaling and does not target STAT2 for degradation

HPIV2 V protein efficiently blocks type I IFN signaling following infection by targeting STAT2 for proteasomal degradation (Andrejeva et al., 2002; Nishio et al., 2002, 2005). Therefore, we determined the effect of deleting the V protein on the ability of HPIV2 to block type I IFN signaling using a biological assay that assesses the establishment of an antiviral state in rHPIV2-infected cells. Vero cells, which do not produce type I IFN, were mock-infected or infected with rHPIV2s at an MOI of 5.0 $TCID_{50}$/cell for 24 h prior to treatment with IFN-β. Twenty-four hours after IFN-β treatment, cells were infected with vesicular stomatitis virus expressing green fluorescent protein (VSV-GFP). The number of VSV-GFP plaques was counted 48 h later, and the percent inhibition of plaque formation due to IFN-β treatment was calculated relative to cells that were not treated with IFN-β (Fig. 4C). In cells that were not infected with HPIV2 (Mock), VSV-GFP replication was inhibited 80% by IFN-β treatment (100 or 1000 IU/ml). The average size (area) of the remaining plaques was reduced approximately 6-fold in IFN-treated wells compared with the size of plaques in untreated wells. In contrast, infection with rHPIV2-WT reduced the inhibitory effect of IFN-β by 75%, i.e. to a level of 20%, indicating that rHPIV2-WT can prevent IFN-β signaling and thereby blunt the induction of an antiviral state. Infection with rHPIV2-V^{ko} was unable to inhibit the antiviral effect of IFN-β resulting in 80% inhibition of VSV-GFP plaque formation in IFN-β-treated cells, identical to that in the mock-infected cultures. The plaque formation by VSV-GFP in cells infected with rHPIV2-V^{ko}, even in the absence of IFN treatment, was inhibited 70% (data not shown), for reasons that are undefined but likely involve the enhanced CPE observed with this virus. Thus, the magnitude of IFN-mediated inhibition associated with this mutant was calculated based on the reduced number of VSV-GFP plaques that form on rHPIV2-V^{ko}-infected monolayers in the absence of added IFN-β.

To investigate whether rHPIV2-V^{ko} was unable to block IFN signaling because it lacked the ability to degrade STAT2, we examined lysates from Vero cells infected with rHPIV2 at an MOI of 5.0 $TCID_{50}$/cell for the expression of STAT1 and STAT2 proteins (Fig. 4D). By 24 hpi, rHPIV2-WT had completely degraded STAT2 in the infected cells and continued to prevent accumulation of STAT2 through 48 hpi. rHPIV2-V^{ko}-infected cells, however, expressed levels of STAT2 that were as high or higher than in mock-infected cells through 48 hpi. Although STAT2 was degraded by rHPIV2-WT and not by rHPIV2-V^{ko}, all infected cell lysates expressed equivalent amounts of STAT1. We also observed that STAT1 could still be phosphorylated in response to IFN-β when we stimulated cells infected with either rHPIV2-WT or rHPIV2-V^{ko} prior to lysis and performed immunoblots using antibodies specific to the phosphorylated form of STAT1 (data not shown). Therefore, rHPIV2-V^{ko} appears to be unable to degrade STAT2, eliminating its ability to block type I IFN signaling, whereas neither rHPIV2-V^{ko} nor rHPIV2-WT appeared to affect STAT1 stability or phosphorylation.

Attenuation of rHPIV2-V^{ko} in vivo

To assess the ability of rHPIV2-V^{ko} to replicate in vivo, we inoculated African green monkeys (AGMs) intranasally (IN) and intratracheally (IT) with 10^6 $TCID_{50}$ of virus per site and determined virus titers from nasopharyngeal swabs (representative of the URT) and tracheal lavage samples (representative of the LRT) (Fig. 5A). rHPIV2-WT replicated to a mean peak titer of $10^{3.5}$ $TCID_{50}$/ml in the URT and approximately 10^4 $TCID_{50}$/ml in the LRT. However, rHPIV2-V^{ko} was undetectable in all of the AGM respiratory tract samples. The lower limit of detection was 0.5 $\log_{10}$ $TCID_{50}$/ml. Likely as a result of its poor replication, rHPIV2-V^{ko} was also poorly immunogenic. While infection of rHPIV2-WT caused a 4.2-fold rise in HPIV2 neutralizing antibody titer in AGMs between day 0 and day 28 p.i., there was no significant rise in response to rHPIV2-V^{ko} (1.5-fold). The poor growth and lack of immunogenicity of rHPIV2-V^{ko} in AGMs indicate that the V protein is required for infection in vivo and suggest that a V-deletion mutant would not make a successful vaccine candidate.

Restricted growth of rHPIV2-V^{ko} in primary human airway epithelial cells (HAE)

As V protein has been implicated in host range restriction of paramyxovirus replication (Parisien et al., 2002; Park et al., 2003), we wanted to determine if replication could be seen in primary epithelial cell cultures of human origin. In vitro models of the human airway epithelium (HAE) can be derived from primary human airway cells grown at an air–liquid interface where they differentiate into a multilayered, polarized epithelium. Unlike transformed monolayer cell lines, these primary polarized epithelial cultures closely mimic morphological and physiological characteristics of the human airway epithelium in vivo, including mucus production and ciliary motion (Matsui et al., 1998; Pickles et al., 1998). The HAE model has been used to investigate characteristics of infection for a number of respiratory viruses, including human coronaviruses, influenza A virus, RSV, HPIV1 and HPIV3 (Bartlett et al., 2008b; Leonard et al., 2008; Sims et al., 2005; Thompson et al., 2006; Zhang et al., 2005, 2002). In the present study, we found that, following apical inoculation of HAE cells with an MOI of 0.01 $TCID_{50}$/cell, rHPIV2-WT replicated efficiently, reaching a peak titer of 10^4 $TCID_{50}$/ml (Fig. 5B). However, as in the AGM samples, rHPIV2-V^{ko} was undetectable in the HAE culture supernatant through day 7 p.i. and appears to be unable to infect HAE productively (Fig. 5B). To determine whether a high level of IFN production limited the growth of rHPIV2-V^{ko} in HAE cultures, we measured the concentration of IFN-β secretion by ELISA (Fig. 5C). A low level of IFN-β was detected in response to rHPIV2-WT infection of HAE (peak of 94 pg/ml on day 4 p.i.). In contrast, cells infected with rHPIV2-V^{ko} showed very little secretion of IFN-β (<20 pg/ml), most likely due to the virus' severely restricted replication.

Discussion

Evaluation of mutants of the Toshiba strain of HPIV2, either containing a deletion of the V-specific cysteine-rich domain, designated as rPIV2V(−) (Kawano et al., 2001), or encoding an alteration of the P editing site that results in ablation of V expression, designated as rPIV2/P-edit (Nishio et al., 2005), indicated that HPIV2 V was required for efficient replication, particularly in IFN-competent cells. We sought to prepare and further characterize an independent V^{ko} HPIV2 to examine the effect of the deletion on the synthesis and signaling of IFN, on cytopathology, and on replication both in vitro and in vivo. To this end, rHPIV2-V^{ko} was generated using a low passage HPIV2 isolate that replicates efficiently in AGMs and that was completely sequenced to confirm its sequence comparability to the WT virus from which it was derived. Since deletion of IFN antagonists such as the NS1/NS2 proteins of influenza virus (Ferko et al., 2004;

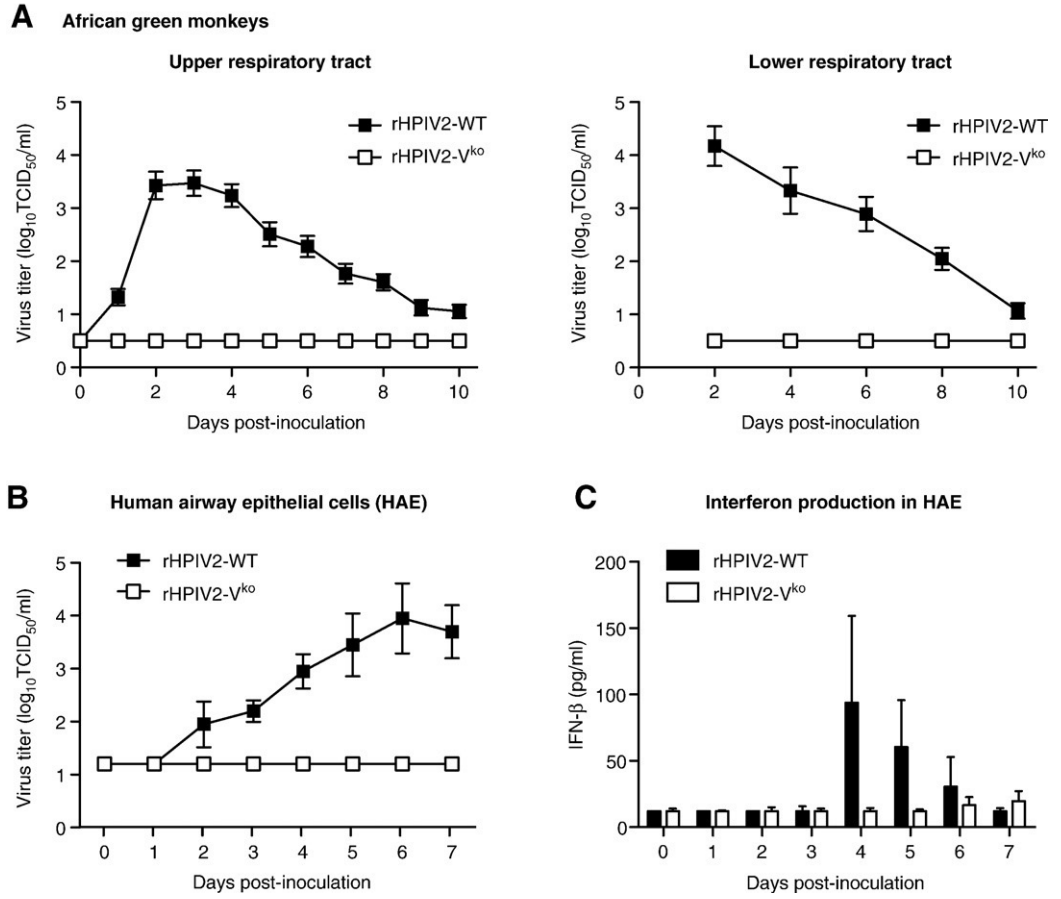

Fig. 5. Restriction of rHPIV2-V^{ko} replication in African green monkeys and an in vitro model of human airway epithelium. (A) Replication in the upper (URT) and lower (LRT) respiratory tract of African green monkeys. Groups of AGMs were inoculated intranasally and intratracheally with 10^6 $TCID_{50}$ of rHPIV2-WT ($n=21$) or rHPIV2-V^{ko} ($n=4$). Mean daily virus titers ± SE in nasopharyngeal swabs (representative of the URT) and tracheal lavage fluid (representative of the LRT) were determined at each indicated sampling day. The limit of detection was 0.5 $\log_{10}$ $TCID_{50}$/ml. (B) Primary polarized human airway epithelial (HAE) tissue cultures, which closely modeled authentic airway epithelium, were infected at the apical surface with rHPIV2-WT or rHPIV2-V^{ko} at low MOI (0.01 $TCID_{50}$/cell). Virus shed into the apical compartment was determined on days 0 to 7 p.i. Virus titers shown are the means of duplicate cultures from two donors ± SE. The limit of detection is 1.2 $\log_{10}TCID_{50}$/ml. (C) IFN-β induction during infection of HAE. Apical wash fluid was analyzed to determine ELISA IFN-β levels, which were determined by comparison with an IFN-β standard curve. IFN-β levels are expressed in pg/ml ± SE based on duplicate samples from two donors; the lower limit of detection was 12 pg/ml.

Hai et al., 2008; Talon et al., 2000) and respiratory syncytial virus (Teng et al., 2000; Whitehead et al., 1999; Wright et al., 2006) can attenuate viruses in vivo and have potential for use as live attenuated virus vaccines, we were particularly interested to see if rHPIV2-V^{ko} had properties suitable for such a vaccine.

rHPIV2-V^{ko} was impaired in replication in vitro, as indicated both by a low frequency of recovery of infectious virus from cDNA and by a considerable restriction of replication in vitro, particularly in IFN-competent LLC-MK2 and A549 cells. rHPIV2-V^{ko} replication in Vero cells, a cell line unable to produce type I IFN (Emeny and Morgan, 1979; Mosca and Pitha, 1986; Wathelet et al., 1992) and also low in constitutive expression of IRF3 (Chew et al., 2009), was 10-fold restricted in peak titer during multi-cycle replication compared to rHPIV2-WT, whereas the previously described rPIV2/P-edit was restricted over 10,000-fold in the same cell line (Nishio et al., 2005). The reason for this difference in replication between the two constructs of rHPIV2-V^{ko} was not defined. It is noteworthy that, in the present study, the entire sequence of the rHPIV2-V^{ko} mutant was analyzed, identifying only a single adventitious mutation. This involved a substitution in the N gene-end signal that changed the length of the poly(A) segment from 7 to 6 residues, a type of change that is common in paramyxoviruses and is usually innocuous (Collins and Crowe, 2007; Kolakofsky et al., 1998; Rassa et al., 2000). This mutation does not alter the length of the untranslated region, and other variable gene-end poly(A) tracts have been demonstrated to be functionally equivalent in directing polyadenylation (Rassa et al., 2000). This virus was largely replication competent and did not reduce the expression of the N and P proteins, suggesting that this single adventitious mutation was inconsequential and that rHPIV2-V^{ko} was a clean V-deletion mutant. It should be noted that there may be increased expression of P protein due to the elimination of RNA editing. This method of ablating V expression removes the possibility of generating a truncated V or W protein but introduces the possibility that greater P expression may also have contributed to the reduction in rHPIV2-V^{ko} replication.

The 10-fold reduction in replication and the reduced plaque size of rHPIV2-V^{ko} versus rHPIV2-WT in Vero cells identified a modest IFN-independent role of V in supporting replication in vitro. A role for V in replication in vitro has been seen with other rubulaviruses and could be due to a recently reported function of V in promoting virus growth through an interaction with the L polymerase (Nishio et al., 2008). A C-terminal truncation mutant of the PIV5 V protein was restricted in replication in IFN-competent cells but grew as efficiently as PIV5 WT in Vero cells, while a PIV5 deletion mutant lacking the entire V protein could not be recovered at all (He et al., 2002). In IFN-competent cells, however, all of the reported rubulavirus V knockout and truncation mutants grow poorly and form pinpoint plaques (He et al., 2002). The severe restriction of replication seen with rubulavirus V knockout and V truncation mutants in IFN-competent cells is not seen with similar V mutants derived from viruses of other paramyxovirus genera

(Delenda et al., 1997; Kato et al., 1997a; Patterson et al., 2000). The respirovirus Sendai virus (SeV), for example, grows efficiently in IFN-competent cells without V protein, suggesting that V is less crucial for replication of respiroviruses than for rubulaviruses (Delenda et al., 1997; Kato et al., 1997a). This likely is because these other genera also possess the accessory C protein, which is not found in rubulaviruses; the functions of the rubulavirus V protein are distributed between the V and C proteins of these other genera. Taken together, these data point toward a role of both IFN-dependent and IFN-independent functions of V in enabling virus replication in vitro.

rHPIV2-V^{ko}-infected cells produced IFN-β efficiently whereas rHPIV2-WT did not, clearly indicating that rHPIV2 V protein inhibits the induction of IFN. All of the paramyxovirus V proteins examined to date have been shown to down-regulate IFN-β induction using a mechanism linked to interaction of the C-terminus of V protein with the helicase domain of MDA5 to block its activation and signaling to IRF3 (Andrejeva et al., 2004; Berghall et al., 2006; Childs et al., 2007, 2009). Although several studies have indicated that RIG-I is the primary helicase for sensing paramyxoviruses rather than MDA5 (Kato et al., 2005, 2006; Loo et al., 2008), the conservation of the V–MDA5 interaction across the four above-mentioned paramyxovirus genera signifies that its role is likely important. Why RIG-I, which does not seem to be a target of paramyxovirus V proteins (Childs et al., 2007; Yoneyama et al., 2005), apparently does not function efficiently in cells infected with rubulaviruses to produce activated IRF3/7 and induce IFN-β remains undefined.

rHPIV2-WT also inhibited the signaling of IFN-β by efficiently degrading STAT2 whereas rHPIV2-V^{ko} did not, confirming previous observations that HPIV2 modulates IFN signaling in human and monkey cells by proteasomal degradation of STAT2 rather than STAT1, which is targeted by rubulaviruses PIV5, SV41 and MuV (Andrejeva et al., 2002; Didcock et al., 1999a, 1999b; Nishio et al., 2005, 2001; Parisien et al., 2001; Precious et al., 2005; Ulane and Horvath, 2002; Ulane et al., 2005; Young et al., 2000). Our demonstration that rHPIV2-WT can degrade STAT2 and block the antiviral effects of IFN-β in AGM-derived Vero cells, while rHPIV2-V^{ko} cannot, supports the use of AGMs as a suitable in vivo model to examine the effect of V on replication in vivo, likely reflecting the observation that human and monkey STAT1 and STAT2 proteins are highly conserved, sharing 99.3% and 97.8% amino acid identity, respectively, between species (Nishio et al., 2005).

rHPIV2-V^{ko} infection induced extensive CPE in vitro whereas rHPIV2-WT was largely non-cytopathic until very late in infection. Several diverse and complex pathways can lead to PIV-induced apoptosis, and V can play a role in preventing apoptosis of infected cells (He et al., 2002; Lei et al., 2009; Peters et al., 2008; Sun et al., 2004; Wansley and Parks, 2002). PIV5 and SeV V mutant viruses, like rHPIV2-V^{ko}, were more cytopathic than their respective WT viruses (Capraro et al., 2008; Kato et al., 1997a). The HPIV2 V truncation mutant induced more cell death in Vero cells than HPIV2-WT (Kawano et al., 2001). In the present study, the mechanism of cell death for rHPIV2-V^{ko}-infected cells was characterized, and the findings indicate that the CPE did not appear to be solely apoptotic in nature. We observed significantly more syncytia formation upon infection with rHPIV2-V^{ko} than with rHPIV2-WT beginning at very early times in infection. Since our rHPIV2-WT and the rHPIV2-V^{ko} mutant are identical in protein sequence except for the V deletion, the difference in syncytia phenotype was not due to differences in sequence of F or HN although changes in F or HN clearly can alter this phenotype (Tsurudome et al., 2008; Yuasa et al., 1995). rHPIV2-V^{ko} exhibited greater necrosis than rHPIV2-WT-infected cells and induced a low level of apoptosis, but the relationship between syncytia formation and necrosis was not further defined. Thus, apoptosis, cell necrosis, and syncytia formation contributed to the enhanced CPE seen with rHPIV2-V^{ko} infection, with necrosis appearing to be a greater contributor than apoptosis.

rHPIV2-V^{ko} was not recovered from the URT and LRT of AGMs, indicating that the V protein is required for detectable replication of HPIV2 in vivo in non-human primates. To address whether this restriction of replication was specific to the organized epithelium of monkeys, i.e., a host range effect that could be specified by the V protein (Parisien et al., 2002; Park et al., 2003), the replication of rHPIV2-V^{ko} was also examined in human organized epithelial cultures. Replication was not seen in the human organized epithelial cells, confirming that HPIV2 V has a profound effect on replication in both human and monkey organized epithelia. The ability of V mutant viruses to exhibit attenuation in vivo has been seen with other paramyxoviruses. A V mutant of PIV5 was restricted in replication in ferrets but not mice, a clear host range difference (Capraro et al., 2008). A measles virus V^{ko} mutant was attenuated in rhesus monkeys, as assessed by the absence of clinical illness and a reduction in the magnitude and duration of viremia (Devaux et al., 2008). Similarly, V protein defective canine distemper virus was restricted 50- to 100-fold in replication in ferrets (von Messling et al., 2006). SeV V mutants that replicated efficiently in vitro were significantly attenuated in mice with a shorter duration of replication and approximately 10-fold lower peak titers than WT SeV (Kato et al., 1997a, 1997b). The greater restriction of rHPIV2-V^{ko} in vivo than morbillivirus or SeV V mutants perhaps is due to V's role as the sole IFN antagonist in HPIV2, whereas measles and SeV have both V and C proteins contributing to IFN antagonism.

The inability of rHPIV2-V^{ko} to replicate to detectable titer in non-human primates and in HAE suggests that this mutant would not be a suitable candidate for development of a live attenuated HPIV2 vaccine, i.e., it is over-attenuated in vivo. Development of a live attenuated HPIV2 vaccine based on loss of the V protein IFN antagonist functions would require that putative IFN antagonist domains in V be altered selectively and that the domains responsible for the protein's functions in genome replication, viral fitness, and virus assembly be defined and remain unaltered in vaccine viruses. We are currently constructing rHPIV2 mutant viruses in which the V and P genes are expressed from separate genes permitting the introduction of mutations in V without affecting P. Only then can the contribution of each individual function of V to attenuation and immunogenicity be assessed and appropriately utilized in HPIV2 vaccine development. Clearly, the loss of all V functions over-attenuates HPIV2 in vivo.

Materials and methods

Cell lines and viruses

Human HEp-2 (ATCC CCL 23) and rhesus monkey LLC-MK2 (ATCC CCL 7.1) cells were maintained in OptiMEM I (Invitrogen, Grand Island, NY) supplemented with 5% FBS and 50 μg/ml gentamicin sulfate. African green monkey Vero cells (ATCC CCL-81) were maintained in MEM (Gibco-Invitrogen) supplemented with 10% FBS, 50 μg/ml gentamicin sulfate and 4 mM L-glutamine. Human A549 cells (ATCC CCL-185) were maintained in F-12 nutrient mixture (Gibco-Invitrogen) supplemented with 10% FBS, 50 μg/ml gentamicin sulfate and 2 mM L-glutamine.

HAE cells were isolated from airway specimens of patients without underlying lung disease. Tissues were provided by the National Disease Research Interchange (NDRI, Philadelphia, PA) or by the UNC Cystic Fibrosis Center Tissue Culture Core as excess tissue following lung transplantation according to protocols approved by the University of North Carolina at Chapel Hill Institutional Review Board. Primary cells derived from single patient sources were first expanded on plastic and then plated on collagen-coated, permeable Transwell-COL (12-mm diameter) supports at a density of 3×10^5 cells per well. HAE cultures were grown in custom media with provision of an air–liquid interface for 4 to 6 weeks to form differentiated, polarized cultures that resemble *in vivo* pseudostratified mucociliary epithelium, as previously described (Pickles et al., 1998).

The HPIV2 recombinants described here (rHPIV2) are based on the biologically derived HPIV2 strain V9412-6 (V94), which was isolated from a nasal wash specimen from an infected infant and was kindly provided by Dr. Peter Wright of Vanderbilt University (Skiadopoulos et al., 2003). The sequence for the V94 strain was determined previously (Genbank accession AF533010). The recombinant wild-type virus, rHPIV2-WT, was previously referred to as rV94(15T) and was derived from an antigenomic cDNA copy of the HPIV2 V94 genome (Nolan et al., 2007). rHPIV2-WT contains a phenotypically silent *Not*I restriction site, which was introduced in the upstream non-translated region of the N gene (HPIV2 nucleotide positions 149–156), and a silent C to T substitution at position 6265 in the coding region of the F gene, as described previously (Nolan et al., 2005; Skiadopoulos et al., 2003). Recombinant vesicular stomatitis virus expressing green fluorescent protein (VSV-GFP) was kindly supplied by John Hiscott (Stojdl et al., 2003) and was propagated in Vero cells.

Plasmid construction

A recombinant HPIV2 virus expressing only P protein from the P/V gene (rHPIV2-V^{ko}) was created by site-directed PCR mutagenesis using the Advantage-HF PCR kit (Clontech Laboratories, Palo Alto, CA). Four unique, silent restriction enzyme sites were inserted into the rHPIV2-WT antigenomic sense cDNA to facilitate incorporation of a P gene containing a mutated editing site: an *Asc*I site at nucleotides 1986–1993 (GCCACACA to GGCGCGCC), *BstE*II and *Age*I sites at nucleotides 3188–3197 (GGTGCAATCA to GGTTACCGGT), and a *Sac*II site at nucleotides 3221–3226 (CCGATC to CCGCGG). Virus recovered by reverse genetics from a plasmid containing these new restriction enzyme sites grew equivalently to rHPIV2-WT in cell culture (data not shown). PCR mutagenesis was then used to modify the RNA editing site from AGGGGGGGAG to AG*A*GG*A*GG*TG*AG (changes underlined) by (i) adding two G residues to shift the reading frame to encode P and (ii) changing three of the seven consecutive G residues to prevent further editing. All mutations were silent in the P ORF. In addition, four nucleotides (TGAC) were inserted in noncoding sequence before the *BstE*II/*Age*I sites to correct for the "rule of six" (Skiadopoulos et al., 2003). All regions of the mutated cDNAs that had been subjected to in vitro polymerase reactions were sequenced using a Perkin-Elmer ABI 3730 sequencer with the BigDye sequencing kit v1.1 (Perkin-Elmer Applied Biosystems, Warrington, UK) as previously described (Newman et al., 2004).

Virus recovery and propagation

rHPIV2-V^{ko} was recovered by reverse genetics in HEp-2 cells and propagated in LLC-MK2 cells as described previously (Nolan et al., 2005; Skiadopoulos et al., 2003). rHPIV2-V^{ko} was biologically cloned by serial terminal dilution on LLC-MK2 cells. To confirm that recovered recombinant viruses contained the introduced mutations, viral RNA was amplified by RT-PCR using the SuperScript First-Strand Synthesis System (Invitrogen) and Advantage-HF PCR kit (Clontech), and its sequence was determined in its entirety as previously described (Newman et al., 2002; Skiadopoulos et al., 2003). Control RT-PCR reactions in which the RT was omitted did not yield amplified product, confirming that the sequence represented viral RNA.

Purified virus stocks were obtained by infection of LLC-MK2 or Vero cells, followed by centrifugation and banding of culture supernatant containing virus in discontinuous 30%/60% (wt/vol) sucrose gradients to minimize contamination by cellular factors such as IFN. Virus titers were determined at 32 °C by serial dilution on LLC-MK2 cells in 96-well plates using hemadsorption with guinea pig erythrocytes to detect infected cultures (Hall et al., 1992; Skiadopoulos et al., 2003). Titers are expressed as $\log_{10}$ $TCID_{50}$/ml (50% tissue culture infectious dose/ml).

Immunoblot analysis of protein expression

Whole cell lysates were prepared by lysing cells (uninfected or at 24, 48, or 72 hpi) in radioimmunoprecipitation assay (RIPA) buffer containing 50 mM Tris (pH 8), 150 mM NaCl, 1% IGEPAL CA-360 (Sigma-Aldrich, St. Louis, MO), 0.1% sodium dodecyl sulfate (SDS) (Open Biosystems, Huntsville, AL), 0.5% deoxycholic acid (Sigma-Aldrich), 50 mM NaF, 1 mM Na_3VO_4, and Complete Mini protease inhibitor tablet (Roche, Indianapolis, IN). Lysates were heated to 70 °C for 10 minutes in 1× NuPAGE LDS sample-loading buffer (Invitrogen) and separated by SDS–polyacrylamide gel electrophoresis (SDS–PAGE) in NuPAGE 4–12% or 10% Bis–Tris gels under denaturing and reducing conditions (Invitrogen). For Native-PAGE analysis of IRF-3 monomers and dimmers, LLC-MK2 cells were lysed in buffer containing 50 mM Tris–HCl (pH 8.0), 150 mM NaCl, 1% IGEPAL CA-360 (Sigma-Aldrich), 50 mM NaF, 5 mM Na_3VO_4, and Complete Mini protease inhibitor tablet (Roche). Native-PAGE was performed using 7% polyacrylamide gels and Tris–glycine running buffer (Bio-Rad, Hercules, CA) containing 0.2% sodium deoxycholate in the cathode chamber (Van Cleve et al., 2006). Gels were first pre-run for 30 min at 40 mA prior to electrophoresis of lysates at 25 mA.

For immunoblotting, proteins were transferred to an Invitrolon PVDF membrane (Invitrogen), blocked in phosphate-buffered saline (PBS) containing 0.1% Tween and 5% milk powder, and incubated with primary antibodies as indicated. Primary antibodies used for immunoblotting were mouse anti-GAPDH-peroxidase (GAPDH-71.1; Sigma-Aldrich), rabbit anti-IRF-3 (FL-425; Santa Cruz Biotechnology, Santa Cruz, CA), rabbit anti-STAT1 (E-23; Santa Cruz Biotechnology), rabbit anti-STAT2 (C-20; Santa Cruz Biotechnology), rabbit anti-phospho(Tyr701)-STAT1 (Chemicon/Millipore, Billerica, MA), and rabbit anti-caspase-3 (Cell Signaling Technology, Danvers, MA). Mouse antibodies to the amino-terminal P/V common region (85A) (Tsurudome et al., 1989) and to the C-terminal V unique region (53-1V) (Nishio et al., 1999) were described previously. A rabbit polyclonal antiserum raised against a synthetic peptide from the HPIV2 N protein amino acids 513–529 (CHEQYRGSQDDDANDATD) was generated by Spring Valley Laboratories, Inc. (Woodbine, MD). Proteins were detected by incubating membranes with horseradish peroxidase-conjugated goat anti-rabbit or goat anti-mouse IgG (KPL, Gaithersburg, MD) and visualized using SuperSignal West Pico Chemiluminescent Substrate (Pierce, Rockford, IL).

Kinetics of rHPIV2-V^{ko} replication

Confluent monolayer cultures of A549, Vero, or LLC-MK2 cells in 6-well plates were infected in triplicate at a multiplicity of infection (MOI) of either 0.01 or 5.0 $TCID_{50}$/cell, as indicated. After incubating for 1 h with virus, cultures were washed three times and incubated at 32 °C. Medium from each well was harvested and replaced with fresh medium at 24 h intervals. Virus present in each sample was quantified by titration on LLC-MK2 cells and detected by hemadsorption. The level of temperature sensitivity of replication was determined by comparing level of rHPIV2-V^{ko} replication to that of rHPIV2-WT at the permissive temperature of 32 °C and at elevated temperatures of 37 °C, 38 °C, 39 °C, and 40 °C as previously described (Nolan et al., 2007; Skiadopoulos et al., 1999).

Plaque size assay

Evaluation of plaque size was performed on Vero or LLC-MK2 cell monolayers incubated at 32 °C. Infected cultures were covered with 0.8% methylcellulose overlay. Ten days p.i., the infected cultures were fixed with 80% methanol, and viral plaques were immunostained using rabbit antiserum raised against purified HPIV2 virus (Spring Valley Laboratories, Inc.) and a goat anti-rabbit secondary antibody conjugated to horseradish peroxidase (KPL). The plaques were

visualized using 4CN 2-component peroxidase substrate (KPL). Plaque size was measured using Adobe Photoshop CS4 software. Mean plaque sizes (in pixels ± standard error, SE) are based on 30 plaques per virus.

Flow cytometry

For detection of caspase-3 activation, LLC-MK2 cells were harvested by scraping at 24, 48, and 72 h after infection with rHPIV2s at an MOI of 5.0 $TCID_{50}$/cell. Cells were washed with PBS, then fixed and permeabilized in BD Cytofix/Cytoperm solution (BD Biosciences, San Diego, CA). After washing in BD Perm/Wash buffer, cells were stained with fluorescein isothiocyanate (FITC)-conjugated monoclonal rabbit anti-active caspase-3 antibody according to the manufacturer's protocol (FITC Active Caspase-3 Apoptosis kit, BD Biosciences).

For detection of cell surface expression of HN and F proteins, LLC-MK2 cells were harvested by trypsinizing at 24 and 48 h after infection with rHPIV2s at an MOI of 5.0 $TCID_{50}$/cell. Cells were washed with PBS and stained with HPIV2-specific antibodies diluted in FACS buffer (PBS, 2% FBS): mouse anti-HN IgG1 (42S1) and mouse anti-F IgG2a (144-1A) (Tsurudome et al., 1989) followed by secondary antibodies anti-mouse IgG1-AlexaFluor 647 and anti-mouse IgG2a AlexaFluor 488 (Invitrogen Molecular Probes). Stained cells were fixed in FACS buffer plus 2% paraformaldehyde prior to analysis. Sample analysis was performed on a FACSCalibur (BD Biosciences) using CellQuestPro software; further analysis was performed using FlowJo software (TreeStar, Inc., Ashland, OR).

Cellular cytotoxicity

Cellular toxicity due to HPIV infection was determined by measuring the amount of lactate dehydrogenase (LDH) leakage into the cell culture media. Media were collected from HPIV-infected LLC-MK2 cell cultures and centrifuged immediately after collection to eliminate cells and cell debris. LDH release was quantified in the supernatants using the Cytotoxicity Detection Kit^{PLUS} (LDH) (Roche) according to the manufacturer's directions. The maximum LDH release (100% cell lysis control) was determined by adding Lysis reagent (Roche) to mock-infected cultures prior to supernatant collection and centrifugation; background LDH release was determined from mock-infected cultures that were not lysed. LDH activity upon reaction with a colorimetric reagent was measured using a microplate reader (VMax, Molecular Devices, Sunnyvale, CA).

IFN-β ELISA

Culture supernatant from LLC-MK2 cells and apical wash fluid from HAE cultures were analyzed for IFN-β levels using the Human Interferon-β ELISA Kit according to the manufacturer's protocol (Fujirebio Inc., Tokyo, Japan). This ELISA kit specifically recognizes the biologically active form of human IFN-β. Absorbance was measured using a microplate reader (VMax, Molecular Devices) and compared to a known concentration of IFN-β standard. IFN concentrations are expressed as means (pg/ml) ± SE. IFN-β ELISA results were verified using a type I IFN bioassay based on the inhibition of VSV-GFP replication, as previously described (Bartlett et al., 2008b; Park et al., 2003).

Type I IFN signaling assay

Vero cells were mock- or rHPIV2-infected at an MOI of 5.0 $TCID_{50}$/cell for 24 h. Cells were then left untreated or treated with 100 or 1000 IU/ml IFN-β (Avonex; Biogen Inc., Cambridge, MA) for 24 h prior to infection with VSV-GFP. VSV-GFP-infected cells were cultured under 0.8% methylcellulose overlay prepared in MEM and supplemented with 50 μg/ml gentamicin sulfate and 4 mM L-glutamine. Plates were read for GFP expression 48 h after VSV-GFP infection using a Typhoon 8600 scanner (Molecular Dynamics), and the number of VSV-GFP-positive foci was counted (Van Cleve et al., 2006).

Evaluation of virus replication in non-human primates

HPIV2-seronegative African green monkeys (AGMs) were inoculated both intranasally (IN) and intratracheally (IT) with 1 ml of L-15 media containing $10^{6.0}$ $TCID_{50}$ of rHPIV2 per site. Nasopharyngeal (NP) swabs were collected on days 0–10 p.i., and tracheal lavage (TL) samples were collected on days 2, 4, 6, 8, and 10 p.i. Virus titers were determined by serial dilution of the samples on LLC-MK2 cells as described above and are expressed as $\log_{10}$ $TCID_{50}$/ml. The lower limit of detection was 0.5 $\log_{10}$ $TCID_{50}$/ml.

Antibody response to HPIV2 was determined by 60% plaque reduction neutralization titer ($PRNT_{60}$) assay on LLC-MK2 cell monolayers for serum samples collected from AGMs on study days 0 and 28 p.i. Test sera were heat inactivated (56 °C for 30 min), and serial 4-fold dilutions beginning at 1:5 were made in OptiMEM supplemented with 5% FBS. rHPIV2-WT, diluted to $10^{3.5}$ $TCID_{50}$/ml, was added to the diluted serum and incubated at 32 °C for 1 h. Virus/Serum mixtures were then added to LLC-MK2 cell monolayers in 24-well plates, rocked for 1 h, and overlaid with 1% methylcellulose in OptiMEM. After incubation at 32 °C for 6 days, cells were fixed in methanol:acetone (50/50) and immunostained using rabbit anti-HPIV2 antiserum and goat anti-rabbit secondary antibody conjugated to horseradish peroxidase (KPL). Plaques were visualized using TrueBlue Peroxidase substrate (KPL).

Virus inoculation of HAE

Prior to inoculation with rHPIV2, the apical surfaces of HAE were rinsed with PBS to remove apical surface secretions and fresh medium was supplied to the basolateral compartments. HAE cultures were inoculated with rHPIV2s at low MOI (0.01 $TCID_{50}$/cell) in 200-μl inocula applied to the apical surface, and the cultures were incubated at 37 °C for 2 h. The apical surfaces of the cultures were then rinsed 3 × 5 min with PBS and returned to the 37 °C incubator. Apical wash samples were collected on days 0–7 p.i. after incubating the apical surface with 400 μl media for 30 min at 37 °C. The apical wash media were recovered and stored at −80 °C until virus titer was determined as described above.

Acknowledgments

We thank Brad Finneyfrock, Robin Kastenmayer, Stacey Miller, and Joanne Swerczek for performing non-human primate studies. We also thank the directors and teams of the UNC Cystic Fibrosis Center Tissue Culture Core, Susan Burkett, Sonja Surman, and Ann-Marie Cruz for technical assistance. John Hiscott of McGill University provided the VSV-GFP virus.

This research was supported by the Intramural Research Program of the NIH, National Institute of Allergy and Infectious Disease, NIH grant R01 HL77844 (RJP), and the NIH Molecular Biology of Viral Diseases Training Grant 5-T32-AI007419. This project was partly performed under a cooperative research and development agreement (CRADA) between NIAID and MedImmune, Inc. (CRADA #AI-5114) for the development of live attenuated virus vaccines for respiratory syncytial viruses, parainfluenza viruses, and human metapneumovirus.

References

Andrejeva, J., Young, D.F., Goodbourn, S., Randall, R.E., 2002. Degradation of STAT1 and STAT2 by the V proteins of simian virus 5 and human parainfluenza virus type 2, respectively: consequences for virus replication in the presence of alpha/beta and gamma interferons. J. Virol. 76 (5), 2159–2167.

Andrejeva, J., Childs, K.S., Young, D.F., Carlos, T.S., Stock, N., Goodbourn, S., Randall, R.E., 2004. The V proteins of paramyxoviruses bind the IFN-inducible RNA helicase, mda-5, and inhibit its activation of the IFN-beta promoter. Proc. Natl. Acad. Sci. U.S.A. 101 (49), 17264–17269.

Bartlett, E.J., Cruz, A.M., Esker, J., Castano, A., Schomacker, H., Surman, S.R., Hennessey, M., Boonyaratanakornkit, J., Pickles, R.J., Collins, P.L., Murphy, B.R., Schmidt, A.C., 2008a. Human parainfluenza virus type 1 C proteins are nonessential proteins that inhibit the host interferon and apoptotic responses and are required for efficient replication in nonhuman primates. J. Virol. 82 (18), 8965–8977.

Bartlett, E.J., Hennessey, M., Skiadopoulos, M.H., Schmidt, A.C., Collins, P.L., Murphy, B.R., Pickles, R.J., 2008b. The role of interferon in the replication of human parainfluenza virus type 1 wild type and mutant viruses in human ciliated airway epithelium. J. Virol. 82 (16), 8059–8070.

Berghall, H., Siren, J., Sarkar, D., Julkunen, I., Fisher, P.B., Vainionpaa, R., Matikainen, S., 2006. The interferon-inducible RNA helicase, mda-5, is involved in measles virus-induced expression of antiviral cytokines. Microbes Infect. 8 (8), 2138–2144.

Capraro, G.A., Johnson, J.B., Kock, N.D., Parks, G.D., 2008. Virus growth and antibody responses following respiratory tract infection of ferrets and mice with WT and P/V mutants of the paramyxovirus Simian Virus 5. Virology 376 (2), 416–428.

Chew, T., Noyce, R., Collins, S.E., Hancock, M.H., Mossman, K.L., 2009. Characterization of the interferon regulatory factor 3-mediated antiviral response in a cell line deficient for IFN production. Mol. Immunol. 46 (3), 393–399.

Childs, K., Stock, N., Ross, C., Andrejeva, J., Hilton, L., Skinner, M., Randall, R., Goodbourn, S., 2007. mda-5, but not RIG-I, is a common target for paramyxovirus V proteins. Virology 359 (1), 190–200.

Childs, K.S., Andrejeva, J., Randall, R.E., Goodbourn, S., 2009. Mechanism of mda-5 Inhibition by paramyxovirus V proteins. J. Virol. 83 (3), 1465–1473.

Collins, P.L., Crowe, J.E., 2007. Respiratory syncytial virus and metapneumovirus, In: Knipe, D.M., Howley, P.M., Griffin, D.E., Lamb, R.A., Martin, M.A., Roizman, B., Strauss, S.E. (Eds.), 5th ed. Fields Virology, Vol. 2. Lippincott Williams&Wilkins, Philadelphia, pp. 1601–1646. 2 vols.

Curran, J., de Melo, M., Moyer, S., Kolakofsky, D., 1991. Characterization of the Sendai virus V protein with an anti-peptide antiserum. Virology 184 (1), 108–116.

Delenda, C., Hausmann, S., Garcin, D., Kolakofsky, D., 1997. Normal cellular replication of Sendai virus without the trans-frame, nonstructural V protein. Virology 228 (1), 55–62.

Devaux, P., Hodge, G., McChesney, M.B., Cattaneo, R., 2008. Attenuation of V- or C-defective measles viruses: infection control by the inflammatory and interferon responses of rhesus monkeys. J. Virol. 82 (11), 5359–5367.

Didcock, L., Young, D.F., Goodbourn, S., Randall, R.E., 1999a. Sendai virus and simian virus 5 block activation of interferon-responsive genes: importance for virus pathogenesis. J. Virol. 73 (4), 3125–3133.

Didcock, L., Young, D.F., Goodbourn, S., Randall, R.E., 1999b. The V protein of simian virus 5 inhibits interferon signalling by targeting STAT1 for proteasome-mediated degradation. J. Virol. 73 (12), 9928–9933.

Emeny, J.M., Morgan, M.J., 1979. Regulation of the interferon system: evidence that Vero cells have a genetic defect in interferon production. J. Gen. Virol. 43 (1), 247–252.

Fensterl, V., Sen, G.C., 2009. Interferons and viral infections. Biofactors 35 (1), 14–20.

Ferko, B., Stasakova, J., Romanova, J., Kittel, C., Sereinig, S., Katinger, H., Egorov, A., 2004. Immunogenicity and protection efficacy of replication-deficient influenza A viruses with altered NS1 genes. J. Virol. 78 (23), 13037–13045.

Goodbourn, S., Didcock, L., Randall, R.E., 2000. Interferons: cell signalling, immune modulation, antiviral response and virus countermeasures. J. Gen. Virol. 81 (Pt 10), 2341–2364.

Hai, R., Martinez-Sobrido, L., Fraser, K.A., Ayllon, J., Garcia-Sastre, A., Palese, P., 2008. Influenza B virus NS1-truncated mutants: live-attenuated vaccine approach. J. Virol. 82 (21), 10580–10590.

Hall, S.L., Stokes, A., Tierney, E.L., London, W.T., Belshe, R.B., Newman, F.C., Murphy, B.R., 1992. Cold-passaged human parainfluenza type 3 viruses contain ts and non-ts mutations leading to attenuation in rhesus monkeys. Virus Res. 22 (3), 173–184.

He, B., Paterson, R.G., Stock, N., Durbin, J.E., Durbin, R.K., Goodbourn, S., Randall, R.E., Lamb, R.A., 2002. Recovery of paramyxovirus simian virus 5 with a V protein lacking the conserved cysteine-rich domain: the multifunctional V protein blocks both interferon-beta induction and interferon signaling. Virology 303 (1), 15–32.

Horvath, C.M., 2004. Weapons of STAT destruction. Interferon evasion by paramyxovirus V protein. Eur. J. Biochem. 271, 4621–4628.

Kapikian, A., Bell, J., Mastrota, F., Huebner, R., Wong, D., Chanock, R., 1963. An outbreak of parainfluenza 2 (croup-associated) virus infection. JAMA 183, 324–330.

Karron, R.A., Collins, P.L., 2007. Chapter 42. Parainfluenza Viruses, In: Knipe, D.M., Howley, P.M. (Eds.), 5th ed. Fields Virology, Vol. 1. Lippincott Williams & Wilkins, Philadelphia, pp. 1497–1526. 2 vols.

Kato, A., Kiyotani, K., Sakai, Y., Yoshida, T., Nagai, Y., 1997a. The paramyxovirus, Sendai virus, V protein encodes a luxury function required for viral pathogenesis. EMBO J. 16 (3), 578–587.

Kato, A., Kiyotani, K., Sakai, Y., Yoshida, T., Shioda, T., Nagai, Y., 1997b. Importance of the cysteine-rich carboxyl-terminal half of V protein for Sendai virus pathogenesis. J. Virol. 71 (10), 7266–7272.

Kato, H., Sato, S., Yoneyama, M., Yamamoto, M., Uematsu, S., Matsui, K., Tsujimura, T., Takeda, K., Fujita, T., Takeuchi, O., Akira, S., 2005. Cell type-specific involvement of RIG-I in antiviral response. Immunity 23 (1), 19–28.

Kato, H., Takeuchi, O., Sato, S., Yoneyama, M., Yamamoto, M., Matsui, K., Uematsu, S., Jung, A., Kawai, T., Ishii, K.J., Yamaguchi, O., Otsu, K., Tsujimura, T., Koh, C.S., Reis e Sousa, C., Matsuura, Y., Fujita, T., Akira, S., 2006. Differential roles of MDA5 and RIG-I helicases in the recognition of RNA viruses. Nature 441 (7089), 101–105.

Kawano, M., Kaito, M., Kozuka, Y., Komada, H., Noda, N., Nanba, K., Tsurudome, M., Ito, M., Nishio, M., Ito, Y., 2001. Recovery of infectious human parainfluenza type 2 virus from cDNA clones and properties of the defective virus without V-specific cysteine-rich domain. Virology 284 (1), 99–112.

Kolakofsky, D., Pelet, T., Garcin, D., Hausmann, S., Curran, J., Roux, L., 1998. Paramyxovirus RNA synthesis and the requirement for hexamer genome length: the rule of six revisited. J. Virol. 72 (2), 891–899.

Koyama, S., Ishii, K.J., Kumar, H., Tanimoto, T., Coban, C., Uematsu, S., Kawai, T., Akira, S., 2007. Differential role of TLR- and RLR-signaling in the immune responses to influenza A virus infection and vaccination. J. Immunol. 179 (7), 4711–4720.

Lamb, R.A., Parks, G., 2007. Paramyxoviridae: the viruses and their replication. 5 ed. In: Fields, B., Knipe, D., Howley, P. (Eds.), "Fields Virology". Lippincott Williams & Wilkins, Philadelphia, pp. 1449–1496.

Lei, Y., Moore, C.B., Liesman, R.M., O'Connor, B.P., Bergstralh, D.T., Chen, Z.J., Pickles, R.J., Ting, J.P., 2009. MAVS-mediated apoptosis and its inhibition by viral proteins. PLoS One 4 (5), e5466.

Leonard, V.H., Sinn, P.L., Hodge, G., Miest, T., Devaux, P., Oezguen, N., Braun, W., McCray Jr., P.B., McChesney, M.B., Cattaneo, R., 2008. Measles virus blind to its epithelial cell receptor remains virulent in rhesus monkeys but cannot cross the airway epithelium and is not shed. J. Clin. Invest. 118 (7), 2448–2458.

Lin, G.Y., Lamb, R.A., 2000. The paramyxovirus simian virus 5 V protein slows progression of the cell cycle. J. Virol. 74 (19), 9152–9166.

Lin, G.Y., Paterson, R.G., Lamb, R.A., 1997. The RNA binding region of the paramyxovirus SV5 V and P proteins. Virology 238 (2), 460–469.

Loo, Y.M., Fornek, J., Crochet, N., Bajwa, G., Perwitasari, O., Martinez-Sobrido, L., Akira, S., Gill, M.A., Garcia-Sastre, A., Katze, M.G., Gale Jr, M., 2008. Distinct RIG-I and MDA5 signaling by RNA viruses in innate immunity. J. Virol. 82 (1), 335–345.

Matsui, H., Grubb, B.R., Tarran, R., Randell, S.H., Gatzy, J.T., Davis, C.W., Boucher, R.C., 1998. Evidence for periciliary liquid layer depletion, not abnormal ion composition, in the pathogenesis of cystic fibrosis airways disease. Cell 95 (7), 1005–1015.

Mosca, J.D., Pitha, P.M., 1986. Transcriptional and posttranscriptional regulation of exogenous human beta interferon gene in simian cells defective in interferon synthesis. Mol. Cell Biol. 6 (6), 2279–2283.

Murphy, B.R., 1988. Current approaches to the development of vaccines effective against parainfluenza viruses. Bull. World Health Organ. 66 (3), 391–397.

Newman, J.T., Surman, S.R., Riggs, J.M., Hansen, C.T., Collins, P.L., Murphy, B.R., Skiadopoulos, M.H., 2002. Sequence analysis of the Washington/1964 strain of human parainfluenza virus type 1 (HPIV1) and recovery and characterization of wild-type recombinant HPIV1 produced by reverse genetics. Virus Genes 24 (1), 77–92.

Newman, J.T., Riggs, J.M., Surman, S.R., McAuliffe, J.M., Mulaikal, T.A., Collins, P.L., Murphy, B.R., Skiadopoulos, M.H., 2004. Generation of recombinant human parainfluenza virus type 1 vaccine candidates by importation of temperature-sensitive and attenuating mutations from heterologous paramyxoviruses. J. Virol. 78 (4), 2017–2028.

Nishio, M., Tsurudome, M., Ito, M., Kawano, M., Kusagawa, S., Komada, H., Ito, Y., 1999. Isolation of monoclonal antibodies directed against the V protein of human parainfluenza virus type 2 and localization of the V protein in virus-infected cells. Med. Microbiol. Immunol. 188 (2), 79–82.

Nishio, M., Tsurudome, M., Ito, M., Kawano, M., Komada, H., Ito, Y., 2001. High resistance of human parainfluenza type 2 virus protein-expressing cells to the antiviral and anti-cell proliferative activities of alpha/beta interferons: cysteine-rich V-specific domain is required for high resistance to the interferons. J. Virol. 75 (19), 9165–9176.

Nishio, M., Garcin, D., Simonet, V., Kolakofsky, D., 2002. The carboxyl segment of the mumps virus V protein associates with Stat proteins in vitro via a tryptophan-rich motif. Virology 300 (1), 92–99.

Nishio, M., Tsurudome, M., Ito, M., Garcin, D., Kolakofsky, D., Ito, Y., 2005. Identification of paramyxovirus V protein residues essential for STAT protein degradation and promotion of virus replication. J. Virol. 79 (13), 8591–8601.

Nishio, M., Tsurudome, M., Ito, M., Ito, Y., 2006. Identification of RNA-binding regions on the P and V proteins of human parainfluenza virus type 2. Medical Microbiological Immunology 195, 29–36.

Nishio, M., Tsurudome, M., Ishihara, H., Ito, M., Ito, Y., 2007. The conserved carboxyl terminus of human parainfluenza virus type 2 V protein plays an important role in virus growth. Virology 362 (1), 85–98.

Nishio, M., Ohtsuka, J., Tsurudome, M., Nosaka, T., Kolakofsky, D., 2008. Human parainfluenza virus type 2 V protein inhibits genome replication by binding to the L protein: possible role in promoting viral fitness. J. Virol. 82 (13), 6130–6138.

Nolan, S.M., Surman, S.R., Amaro-Carambot, E., Collins, P.L., Murphy, B.R., Skiadopoulos, M.H., 2005. Live-attenuated intranasal parainfluenza virus type 2 vaccine candidates developed by reverse genetics containing L polymerase protein mutations imported from heterologous paramyxoviruses. Vaccine 39 (23), 4765–4774.

Nolan, S.M., Skiadopoulos, M.H., Bradley, K., Kim, O.S., Bier, S., Amaro-Carambot, E., Surman, S.R., Davis, S., St Claire, M., Elkins, R., Collins, P.L., Murphy, B.R., Schaap-Nutt, A., 2007. Recombinant human parainfluenza virus type 2 vaccine candidates containing a 3′ genomic promoter mutation and L polymerase mutations are attenuated and protective in non-human primates. Vaccine 25 (34), 6409–6422.

Ohgimoto, S., Bando, H., Kawano, M., Okamoto, K., Kondo, K., Tsurudome, M., Nishio, M., Ito, Y., 1990. Sequence analysis of P gene of human parainfluenza type 2 virus: P and cysteine-rich proteins are translated by two mRNAs that differ by two nontemplated G residues. Virology 177 (1), 116–123.

Parisien, J.P., Lau, J.F., Rodriguez, J.J., Sullivan, B.M., Moscona, A., Parks, G.D., Lamb, R.A., Horvath, C.M., 2001. The V protein of human parainfluenza virus 2 antagonizes type I interferon responses by destabilizing signal transducer and activator of transcription 2. Virology 283 (2), 230–239.

Parisien, J.P., Lau, J.F., Horvath, C.M., 2002. STAT2 acts as a host range determinant for species-specific paramyxovirus interferon antagonism and simian virus 5 replication. J. Virol. 76 (13), 6435–6441.

Park, M.S., Garcia-Sastre, A., Cros, J.F., Basler, C.F., Palese, P., 2003. Newcastle disease virus V protein is a determinant of host range restriction. J. Virol. 77 (17), 9522–9532.
Parrott, R., Vargosko, A., HW, K., Bell, J., Chanock, R., 1962. Myxoviruses. III. Parainfluenza. Am. J. Public Health 52, 907–917.
Paterson, R., Leser, G., Shaughnessy, M., Lamb, R., 1995. The paramyxovirus SV5 V protein binds two atoms of zinc and is a structural component of virions. Virology 208, 121–131.
Patterson, J.B., Thomas, D., Lewicki, H., Billeter, M.A., Oldstone, M.B., 2000. V and C proteins of measles virus function as virulence factors in vivo. Virology 267 (1), 80–89.
Peters, K., Chattopadhyay, S., Sen, G.C., 2008. IRF-3 activation by Sendai virus infection is required for cellular apoptosis and avoidance of persistence. J. Virol. 82 (7), 3500–3508.
Pickles, R.J., McCarty, D., Matsui, H., Hart, P.J., Randell, S.H., Boucher, R.C., 1998. Limited entry of adenovirus vectors into well-differentiated airway epithelium is responsible for inefficient gene transfer. J. Virol. 72 (7), 6014–6023.
Poole, E., He, B., Lamb, R.A., Randall, R.E., Goodbourn, S., 2002. The V proteins of Simian virus 5 and other paramyxoviruses inhibit induction of interferon-beta. Virology 303 (1), 33–46.
Precious, B., Young, D.F., Andrejeva, L., Goodbourn, S., Randall, R.E., 2005. In vitro and in vivo specificity of ubiquitination and degradation of STAT1 and STAT2 by the V proteins of the paramyxoviruses simian virus 5 and human parainfluenza virus type 2. J. Gen. Virol. 86 (Pt 1), 151–158.
Randall, R.E., Bermingham, A., 1996. NP:P and NP:V interactions of the paramyxovirus simian virus 5 examined using a novel protein:protein capture assay. Virology 224 (1), 121–129.
Rassa, J.C., Wilson, G.M., Brewer, G.A., Parks, G.D., 2000. Spacing constraints on reinitiation of paramyxovirus transcription: the gene end U tract acts as a spacer to separate gene end from gene start sites. Virology 274 (2), 438–449.
Sims, A.C., Baric, R.S., Yount, B., Burkett, S.E., Collins, P.L., Pickles, R.J., 2005. Severe acute respiratory syndrome coronavirus infection of human ciliated airway epithelia: role of ciliated cells in viral spread in the conducting airways of the lungs. J. Virol. 79 (24), 15511–15524.
Skiadopoulos, M.H., Tao, T., Surman, S.R., Collins, P.L., Murphy, B.R., 1999. Generation of a parainfluenza virus type 1 vaccine candidate by replacing the HN and F glycoproteins of the live-attenuated PIV3 cp45 vaccine virus with their PIV1 counterparts. Vaccine 18 (5-6), 503–510.
Skiadopoulos, M.H., Vogel, L., Riggs, J.M., Surman, S.R., Collins, P.L., Murphy, B.R., 2003. The genome length of human parainfluenza virus type 2 follows the rule of six, and recombinant viruses recovered from non-polyhexameric-length antigenomic cDNAs contain a biased distribution of correcting mutations. J. Virol. 77 (1), 270–279.
Stojdl, D.F., Lichty, B.D., tenOever, B.R., Paterson, J.M., Power, A.T., Knowles, S., Marius, R., Reynard, J., Poliquin, L., Atkins, H., Brown, E.G., Durbin, R.K., Durbin, J.E., Hiscott, J., Bell, J.C., 2003. VSV strains with defects in their ability to shutdown innate immunity are potent systemic anti-cancer agents. Cancer Cell 4 (4), 263–275.
Sun, M., Rothermel, T.A., Shuman, L., Aligo, J.A., Xu, S., Lin, Y., Lamb, R.A., He, B., 2004. Conserved cysteine-rich domain of paramyxovirus simian virus 5 V protein plays an important role in blocking apoptosis. J. Virol. 78 (10), 5068–5078.
Talon, J., Salvatore, M., O'Neill, R.E., Nakaya, Y., Zheng, H., Muster, T., Garcia-Sastre, A., Palese, P., 2000. Influenza A and B viruses expressing altered NS1 proteins: a vaccine approach. Proc. Natl. Acad. Sci. U. S. A. 97 (8), 4309–4314.
Teng, M.N., Whitehead, S.S., Bermingham, A., St Claire, M., Elkins, W.R., Murphy, B.R., Collins, P.L., 2000. Recombinant respiratory syncytial virus that does not express the NS1 or M2-2 protein is highly attenuated and immunogenic in chimpanzees. J. Virol. 74 (19), 9317–9321.
Thompson, C.I., Barclay, W.S., Zambon, M.C., Pickles, R.J., 2006. Infection of human airway epithelium by human and avian strains of influenza a virus. J. Virol. 80 (16), 8060–8068.
Tsurudome, M., Nishio, M., Komada, H., Bando, H., Ito, Y., 1989. Extensive antigenic diversity among human parainfluenza type 2 virus isolates and immunological relationships among paramyxoviruses revealed by monoclonal antibodies. Virology 171 (1), 38–48.
Tsurudome, M., Nishio, M., Ito, M., Tanahashi, S., Kawano, M., Komada, H., Ito, Y., 2008. Effects of hemagglutinin-neuraminidase protein mutations on cell–cell fusion mediated by human parainfluenza type 2 virus. J. Virol. 82 (17), 8283–8295.
Ulane, C.M., Horvath, C.M., 2002. Paramyxoviruses SV5 and HPIV2 assemble STAT protein ubiquitin ligase complexes from cellular components. Virology 304 (2), 160–166.
Ulane, C.M., Kentsis, A., Cruz, C.D., Parisien, J.P., Schneider, K.L., Horvath, C.M., 2005. Composition and assembly of STAT-targeting ubiquitin ligase complexes: paramyxovirus V protein carboxyl terminus is an oligomerization domain. J. Virol. 79 (16), 10180–10189.
Van Cleve, W., Amaro-Carambot, E., Surman, S.R., Bekisz, J., Collins, P.L., Zoon, K.C., Murphy, B.R., Skiadopoulos, M.H., Bartlett, E.J., 2006. Attenuating mutations in the P/C gene of human parainfluenza virus type 1 (HPIV1) vaccine candidates abrogate the inhibition of both induction and signaling of type I interferon (IFN) by wild-type HPIV1. Virology 352 (1), 61–73.
von Messling, V., Svitek, N., Cattaneo, R., 2006. Receptor (SLAM [CD150]) recognition and the V protein sustain swift lymphocyte-based invasion of mucosal tissue and lymphatic organs by a morbillivirus. J. Virol. 80 (12), 6084–6092.
Wansley, E.K., Parks, G.D., 2002. Naturally occurring substitutions in the p/v gene convert the noncytopathic paramyxovirus simian virus 5 into a virus that induces alpha/beta interferon synthesis and cell death. J. Virol. 76 (20), 10109–10121.
Wathelet, M.G., Berr, P.M., Huez, G.A., 1992. Regulation of gene expression by cytokines and virus in human cells lacking the type-I interferon locus. Eur. J. Biochem. 206 (3), 901–910.
Whitehead, S.S., Bukreyev, A., Teng, M.N., Firestone, C.Y., St Claire, M., Elkins, W.R., Collins, P.L., Murphy, B.R., 1999. Recombinant respiratory syncytial virus bearing a deletion of either the NS2 or SH gene is attenuated in chimpanzees. J. Virol. 73 (4), 3438–3442.
Wright, P.F., Karron, R.A., Madhi, S.A., Treanor, J.J., King, J.C., O'Shea, A., Ikizler, M.R., Zhu, Y., Collins, P.L., Cutland, C., Randolph, V.B., Deatly, A.M., Hackell, J.G., Gruber, W.C., Murphy, B.R., 2006. The interferon antagonist NS2 protein of respiratory syncytial virus is an important virulence determinant for humans. J. Infect. Dis. 193 (4), 573–581.
Yoneyama, M., Fujita, T., 2007. Function of RIG-I-like receptors in antiviral innate immunity. J. Biol. Chem. 282 (21), 15315–15318.
Yoneyama, M., Suhara, W., Fukuhara, Y., Fukuda, M., Nishida, E., Fujita, T., 1998. Direct triggering of the type I interferon system by virus infection: activation of a transcription factor complex containing IRF-3 and CBP/p300. EMBO J. 17 (4), 1087–1095.
Yoneyama, M., Kikuchi, M., Natsukawa, T., Shinobu, N., Imaizumi, T., Miyagishi, M., Taira, K., Akira, S., Fujita, T., 2004. The RNA helicase RIG-I has an essential function in double-stranded RNA-induced innate antiviral responses. Nat. Immunol. 5 (7), 730–737.
Yoneyama, M., Kikuchi, M., Matsumoto, K., Imaizumi, T., Miyagishi, M., Taira, K., Foy, E., Loo, Y.M., Gale Jr., M., Akira, S., Yonehara, S., Kato, A., Fujita, T., 2005. Shared and unique functions of the DExD/H-box helicases RIG-I, MDA5, and LGP2 in antiviral innate immunity. J. Immunol. 175 (5), 2851–2858.
Young, D.F., Didcock, L., Goodbourn, S., Randall, R.E., 2000. Paramyxoviridae use distinct virus-specific mechanisms to circumvent the interferon response. Virology 269 (2), 383–390.
Yuasa, T., Kawano, M., Tabata, N., Nishio, M., Kusagawa, S., Komada, H., Matsumura, H., Ito, Y., Tsurudome, M., 1995. A cell fusion-inhibiting monoclonal antibody binds to the presumed stalk domain of the human parainfluenza type 2 virus hemagglutinin-neuraminidase protein. Virology 206 (2), 1117–1125.
Zhang, L., Peeples, M.E., Boucher, R.C., Collins, P.L., Pickles, R.J., 2002. Respiratory syncytial virus infection of human airway epithelial cells is polarized, specific to ciliated cells, and without obvious cytopathology. J. Virol. 76 (11), 5654–5666.
Zhang, L., Bukreyev, A., Thompson, C.I., Watson, B., Peeples, M.E., Collins, P.L., Pickles, R.J., 2005. Infection of ciliated cells by human parainfluenza virus type 3 in an in vitro model of human airway epithelium. J. Virol. 79 (2), 1113–1124.